

# **The ABCflux database: Arctic-Boreal CO<sub>2</sub> flux observations and ancillary information aggregated to monthly time steps across terrestrial ecosystems**

Authors: Anna-Maria Virkkala<sup>1</sup>, Susan M. Natali<sup>1</sup>, Brendan M. Rogers<sup>1</sup>, Jennifer D. Watts<sup>1</sup>, Kathleen Savage<sup>1</sup>, Sara June Connon<sup>1</sup>, Marguerite Mauritz<sup>2</sup>, Edward A.G. Schuur<sup>3</sup>, Darcy Peter<sup>1</sup>, Christina Minions<sup>1</sup>, Julia Nojeim<sup>1</sup>, Roisin Commane<sup>4</sup>, Craig A. Emmerton<sup>5</sup>, Mathias Goeckede<sup>6</sup>, Manuel Helbig<sup>7,8</sup>, David Holl<sup>9</sup>, Hiroki Iwata<sup>10</sup>, Hideki Kobayashi<sup>11</sup>, Pasi Kolari<sup>12</sup>, Efrén López-Blanco<sup>13,14</sup>, Maija E. Marushchak<sup>15,16</sup>, Mikhail Mastepanov<sup>14,17</sup>, Lutz Merbold<sup>18</sup>, Frans-Jan W. Parmentier<sup>19,20</sup>, Matthias Peichl<sup>21</sup>, Torsten Sachs<sup>22</sup>, Oliver Sonnentag<sup>8</sup>, Masahito Ueyama<sup>23</sup>, Carolina Voigt<sup>15,8</sup>, Mika Aurela<sup>24</sup>, Julia Boike<sup>25,26</sup>, Gerardo Celis<sup>27</sup>, Namyi Chae<sup>28</sup>, Torben R. Christensen<sup>14</sup>, M. Sydonia Bret-Harte<sup>29</sup>, Sigrid Dengel<sup>30</sup>, Han Dolman<sup>31</sup>, Colin W. Edgar<sup>29</sup>, Bo Elberling<sup>32</sup>, Eugenie Euskirchen<sup>29</sup>, Achim Grelle<sup>33</sup>, Juha Hatakka<sup>24</sup>, Elyn Humphreys<sup>34</sup>, Järvi Järveoja<sup>21</sup>, Ayumi Kotani<sup>35</sup>, Lars Kutzbach<sup>9</sup>, Tuomas Laurila<sup>24</sup>, Annalea Lohila<sup>24,12</sup>, Ivan Mammarella<sup>12</sup>, Yojiro Matsuura<sup>36</sup>, Gesa Meyer<sup>8,37</sup>, Mats B. Nilsson<sup>21</sup>, Steven F. Oberbauer<sup>38</sup>, Sang-Jong Park<sup>39</sup>, Roman Petrov<sup>40</sup>, Anatoly S. Prokushkin<sup>41</sup>, Christopher Schulze<sup>8,42</sup>, Vincent L. St.Louis<sup>5</sup>, Eeva-Stiina Tuittila<sup>43</sup>, Juha-Pekka Tuovinen<sup>24</sup>, William Quinton<sup>44</sup>, Andrej Varlagin<sup>45</sup>, Donatella Zona<sup>46</sup>, Viacheslav I. Zyrjanov<sup>41</sup>

1 Woodwell Climate Research Center, 149 Woods Hole Road Falmouth, MA, 02540-1644, USA

2 University of Texas, at El Paso, 500 W University Rd, El Paso, TX 79902, USA

3 Center for Ecosystem Science and Society, and Department of Biological Sciences, Northern Arizona University, Flagstaff, AZ, 86001

4 Dept. of Earth & Environmental Sciences, Lamont-Doherty Earth Observatory, Columbia University, Palisades, NY 10964

5 Department of Biological Sciences, University of Alberta, Edmonton, Alberta, Canada T6G 2E9

6 Dept. Biogeochemical Signals, Max Planck Institute for Biogeochemistry, Jena, Germany

7 Department of Physics and Atmospheric Science, Dalhousie University, Halifax, Nova Scotia, Canada

8 Departement de Geographie, Universite de Montreal, Montreal, Quebec, Canada

9 Institute of Soil Science, Center for Earth System Research and Sustainability (CEN), Universität Hamburg, Hamburg, Germany

10 Department of Environmental Science, Shinshu University, Matsumoto, Japan

11 Research Institute for Global Change, Japan Agency for Marine-Earth Science and Technology, Yokohama, Japan

12 Institute for Atmospheric and Earth System Research/Physics, Faculty of Science, University of Helsinki, Finland

13 Department of Environment and Minerals, Greenland Institute of Natural Resources, Kivioq 2, 3900, Nuuk, Greenland

14 Department of Bioscience, Arctic Research Center, Aarhus University, Frederiksborgvej 399, 4000 Roskilde, Denmark

15 Department of Environmental and Biological Sciences, University of Eastern Finland, Kuopio, Finland

16 Department of Biological and Environmental Science, University of Jyväskylä, Jyväskylä, Finland

17 Oulanka research station, University of Oulu, Liikasenvaarantie 134, 93900 Kuusamo, Finland

18 Agroscope, Research Division Agroecology and Environment, Reckenholzstrasse 191, 8046 Zurich, Switzerland

19 Center for Biogeochemistry in the Anthropocene, Department of Geosciences, University of Oslo, 0315 Oslo, Norway

20 Department of Physical Geography and Ecosystem Science, Lund University, 223 62 Lund, Sweden

21 Department of Forest Ecology and Management, Swedish University of Agricultural Sciences, 901 83 Umeå, Sweden

22 GFZ German Research Centre for Geosciences, Telegrafenberg, Potsdam, Germany

23 Graduate School of Life and Environmental Sciences, Osaka Prefecture University, 1-1 Gakuencho, Naka-ku, Sakai, 599-8531, Japan

24 Finnish Meteorological Institute, Climate system research, Helsinki, Finland

25 Alfred Wegener Institute Helmholtz Center for Polar and Marine Research, Telegrafenberg A45, 14473 Potsdam, Germany & Geography Department, Humboldt-Universität zu Berlin, Unter den Linden 6, 10099 Berlin, Germany

26 Geography Department, Humboldt-Universität zu Berlin, Berlin, Germany

27 Agronomy Department, University of Florida, Gainesville, USA

28 Institute of Life Science and Natural Resources, Korea University, 145 Anam-ro, Seongbuk-gu, Seoul, 02841, Republic of Korea

29 Institute of Arctic Biology, University of Alaska Fairbanks, Fairbanks, AK 99775, USA

30 Earth and Environmental Sciences Area. Lawrence Berkeley National Lab, Berkeley, CA 94720, USA

31 Department of Earth Sciences, VU University of Amsterdam, Amsterdam, The Netherlands

32 Center for Permafrost, Department of Geosciences and Natural Resource Management, University of Copenhagen, Øster Voldgade 10

33 Department of Ecology, Swedish University of Agricultural Sciences, Uppsala

34 Department of Geography & Environmental Studies, Carleton University, 1125 Colonel By Dr. Ottawa, ON, K2B 5J5 Canada

35 Graduate School of Bioagricultural Sciences, Nagoya University, Nagoya, Japan

36 Forestry and Forest Products Research Institute

37 Environment and Climate Change Canada, Climate Research Division, Victoria, BC V8N 1V8, Canada

38 Department of Biological Sciences and Institute of Environment, Florida International University, Miami Florida 33199 USA

39 Division of Atmospheric Sciences, Korea Polar Research Institute, 26 Songdomirae-ro Yeosu-gu, Incheon, Republic of Korea 21990

40 Institute for Biological Problems of Cryolithozone of the Siberian Branch of the RAS - Division of Federal Research Centre "The Yakut Scientific Centre of the Siberian Branch of the Russian Academy of Sciences

41 VN Sukachev Institute of forest SB RAS, Akademgorodok 50/28, Krasnoyarsk 660036 Russia

42 Department of Renewable Resources, University of Alberta, Edmonton, Alberta, Canada T6G 2E9

43 School of Forest Sciences, University of Eastern Finland, Finland

44 Cold Regions Research Centre, Wilfrid Laurier University, Waterloo, Ontario, Canada, N2L 3C5

45 A.N. Severtsov Institute of Ecology and Evolution, Russian Academy of Sciences, 119071, Leninsky pr.33, Moscow, Russia

46 Department of Biology, San Diego State University

ORCID iDs:

AMV: 0000-0003-4877-2918

SMN: 0000-0002-3010-2994

BMR: 0000-0001-6711-8466

MaM: 0000-0001-8733-9119

EAGS: 0000-0002-1096-2436

RC: 0000-0003-1373-1550

MG: 0000-0003-2833-8401  
MH: 0000-0003-1996-8639  
DH: 0000-0002-9269-7030  
HI: 0000-0002-8962-8982  
HK: 0000-0001-9319-0621  
PK: 0000-0001-7271-633X  
ELB: 0000-0002-3796-8408  
MEM: 0000-0002-2308-5049  
MiM: 0000-0002-5543-0302  
LM: 0000-0003-4974-170X  
FJP: 0000-0003-2952-7706  
MP: 0000-0002-9940-5846  
TS: 0000-0002-9959-4771  
MU: 0000-0002-4000-4888  
CV: 0000-0001-8589-1428  
MA: 0000-0002-4046-7225  
JB: 0000-0002-5875-2112  
GC: 0000-0003-1265-4063  
TRC: 0000-0002-4917-148X  
MSB: 0000-0001-5151-3947  
SD: 0000-0002-4774-9188  
CE: 0000-0002-7026-8358  
BE: 0000-0002-6023-885X

SEE: 0000-0002-0848-4295  
AG: 0000-0003-3468-9419  
EH: 0000-0002-5397-2802  
JJ: 0000-0001-6317-660X  
AK: 0000-0003-0350-0775  
LK: /0000-0003-2631-2742  
TL: 0000-0002-1967-0624  
AL: 0000-0003-3541-672X  
IM: 0000-0002-8516-3356  
GM: 0000-0003-3199-5250  
MBN: 0000-0003-3765-6399  
SFO: 0000-0001-5404-1658  
SJP: 0000-0002-6944-6962  
RP: 0000-0002-6877-3902  
ASP: 0000-0001-8721-2142  
CS: 0000-0002-6579-0360  
VLStL: 0000-0001-5405-1522  
EST: 0000-0001-8861-3167  
JPT: 0000-0001-7857-036X  
WQ: 0000-0001-5707-4519  
DZ: 0000-0002-0003-4839  
VIZ: 0000-0002-1748-4801  
AV: 0000-0002-2549-5236

CAE: 0000-0001-9511-9191

Word count: 9200 (abstract: [330302](#), main text: [6400~6900](#))

Corresponding author: Anna-Maria Virkkala, [avirkkala@woodwellclimate.org](mailto:avirkkala@woodwellclimate.org)

## Abstract

Past efforts to synthesize and quantify the magnitude and change in carbon dioxide (CO<sub>2</sub>) fluxes in terrestrial ecosystems across the rapidly warming Arctic-Boreal Zone (ABZ) have provided valuable information, but were limited in their geographical and temporal coverage. Furthermore, these efforts have been based on data aggregated over varying time periods, often with only minimal site ancillary data, thus limiting their potential to be used in large-scale carbon budget assessments. To bridge these gaps, we developed a standardized monthly database of Arctic-Boreal CO<sub>2</sub> fluxes (ABCflux) that aggregates *in-situ* measurements of terrestrial net ecosystem CO<sub>2</sub> exchange and its derived partitioned component fluxes: gross primary productivity and ecosystem respiration. The data span from 1989 to 2020 with over 70 supporting variables that describe key site conditions (e.g., vegetation and disturbance type), micrometeorological and environmental measurements (e.g., air and soil temperatures) and flux measurement techniques. Here, we describe these variables, the spatial and temporal distribution of observations, the main strengths and limitations of the database, and the potential research opportunities it enables. In total, ABCflux includes 244 sites and 6309 monthly observations; 136 sites and 2217 monthly observations represent tundra, and 108 sites and 4092 observations represent the boreal biome. The database includes fluxes estimated with chamber (19 % of the monthly observations), snow diffusion (3 %) and eddy covariance (78 %) techniques. The largest number of observations were collected during the climatological summer (June-August; 32 %), and fewer observations were available for autumn (September-October; 25 %), winter (December-February; 18 %), and spring (March-May; 25 %).

ABCflux can be used in a wide array of empirical, remote sensing and modeling studies to improve understanding of the regional and temporal variability in CO<sub>2</sub> fluxes, and to better estimate the terrestrial ABZ CO<sub>2</sub> budget. ABCflux is openly and freely available online (<https://doi.org/10.3334/ORNLDAAAC/1934>, Virkkala et al., 2021a).

## 1. Introduction

The Arctic-Boreal Zone (ABZ), comprising the northern tundra and boreal biomes, stores approximately half the global soil organic carbon pool (Hugelius et al., 2014; Tarnocai et al., 2009; Mishra et al., 2021). As indicated by this large carbon reservoir, the ABZ has acted as a carbon sink over the past millenia due to the cold climate and slow decomposition rates (Siewert et al., 2015; Hugelius et al., 2020; Gorham, 1991). However, these carbon stocks are increasingly vulnerable to climate change, which is occurring rapidly across the ABZ (Box et al., 2019). As a result, carbon is being lost from this reservoir to the atmosphere as carbon dioxide (CO<sub>2</sub>) through increased ecosystem respiration (Reco) (Schuur et al., 2015; Parker et al., 2015; Voigt et al., 2017). The impact of increased CO<sub>2</sub> emissions on global warming depends on the extent to which respiratory losses are offset by gross primary productivity (GPP), the vegetation uptake of atmospheric CO<sub>2</sub> via photosynthesis (McGuire et al., 2016; Cahoon et al., 2016).



Carbon dioxide flux measurements provide a means to monitor the net CO<sub>2</sub> balance (i.e., net ecosystem exchange; NEE, a balance between GPP and Reco) across time and space (Baldocchi, 2008; Pavelka et al., 2018). There are three main techniques used to measure fluxes at the ecosystem level that represent fluxes from plants and soils [to the atmosphere](#): eddy covariance, automated and manual chambers, and snow diffusion methods (hereafter diffusion; for a comparison of the techniques, see Table 1 in McGuire et al. 2012). The eddy covariance technique estimates NEE at the ecosystem scale (ca. 0.01 to 1 km<sup>2</sup> footprint) at high temporal resolution (i.e., ½ hr) using nondestructive and automated measurements (Pastorello et al., 2020). Automated and manual chamber techniques measure NEE at fine spatial scales (< 1 m<sup>2</sup>) and in small-statured ecosystems, common in the tundra, where the chambers can fit over the whole plant community (Järveoja et al., 2018; López-Blanco et al., 2017). The diffusion technique, [also operating at fine spatial scales](#), can be used to measure the transport of CO<sub>2</sub> within a snowpack (Björkman et al., 2010b). The eddy covariance technique has been used globally for over three decades, and chamber and diffusion techniques for even longer.

Historically, the number and distribution of ABZ flux sites has been rather limited compared to observations in temperate regions (Baldocchi et al., 2018). Due to these data gaps, quantifying the net annual CO<sub>2</sub> balance across the ABZ has posed a significant challenge (Natali et al., [2019](#)[2019a](#); McGuire et al., 2016; Virkkala et al., [2021b](#)[2021](#)). However, over the past decade, the availability of ABZ flux data has increased substantially. Many, but not all, of the ABZ eddy covariance sites are a part of broader networks, such as the global FLUXNET and regional AmeriFlux, Integrated Carbon Observation System (ICOS) and the European Fluxes Database Cluster (EuroFlux), where data are standardized and openly available (Paris et al., 2012; Novick et al., 2018; Pastorello et al., 2020). These networks primarily include flux and meteorological data, but do not often include other environmental descriptions such as soil carbon stocks, dominant plant species, or the disturbance history of a given site (but see, for example, [BADMBiological, Ancillary, Disturbance, and Metadata](#) data in Ameriflux), which are important for understanding the controls on CO<sub>2</sub> fluxes. Moreover, even though some ABZ annual chamber measurements are included in the global soil respiration database (SRDB) (Jian et al., 2020), and in the continuous soil respiration database (COSORE) (Bond-Lamberty et al., 2020),

standardized datasets providing ABZ CO<sub>2</sub> flux measurements from eddy covariance, chambers, and diffusion, along with comprehensive metadata, have been nonexistent. Such an effort would create potential for a more thorough understanding of ABZ CO<sub>2</sub> fluxes. Therefore, compiling these flux measurements and their supporting ancillary data into one database is clearly needed to support future modeling, remote sensing, and empirical data mining efforts.

Arctic-Boreal CO<sub>2</sub> fluxes have been previously synthesized in a handful of regional studies (Belshe et al., 2013; McGuire et al., 2012; Luysaert et al., 2007; Baldocchi et al., 2018; Virkkala et al., 2018; Natali et al., [2019](#)[2019a](#); Virkkala et al., 2021b) (Fig. 1 and Table 1). One of the main challenges in these previous efforts, in addition to the limited geographical coverage of ABZ sites and lack of environmental descriptions, has been the variability of the synthesized seasonal measurement periods. Most of these efforts have allowed the seasonal definitions and measurement periods to vary across the sites, creating uncertainty in the inter-site comparison of flux measurements. An alternative approach to define seasonality is to focus on standard time periods such as months (Natali et al., [2019](#)[2019a](#)). Although focusing on monthly fluxes may result in a small decrease in synthesizable data, because publications, particularly older ones, often provide seasonal rather than monthly flux estimates (see e.g., (Euskirchen et al., 2012; Nykänen et al., 2003; Björkman et al., 2010a; Oechel et al., 2000; Merbold et al., 2009)), compiling monthly fluxes has several advantages over the seasonal fluxes. These advantages include: (i) better comparability of measurements, (ii) ability to bypass problems related to defining seasons across large regions, and (iii) ease of linking these fluxes to remote sensing and models.

Our goal is to build upon past synthesis efforts and compile a new database of Arctic-Boreal CO<sub>2</sub> fluxes (ABCflux version 1) that combines eddy covariance, chamber, and diffusion data at monthly timescales with supporting environmental information to help facilitate large-scale assessments of the ABZ carbon cycle. This paper provides a general description of the ABCflux database by characterizing the data sources and database structure (Section 2), as well as describing the characteristics of the database (Section 3). Additionally, we describe the main

strengths, limitations, and opportunities of this database (Section 4), and its potential utility for future studies aiming to understand terrestrial ABZ CO<sub>2</sub> fluxes.

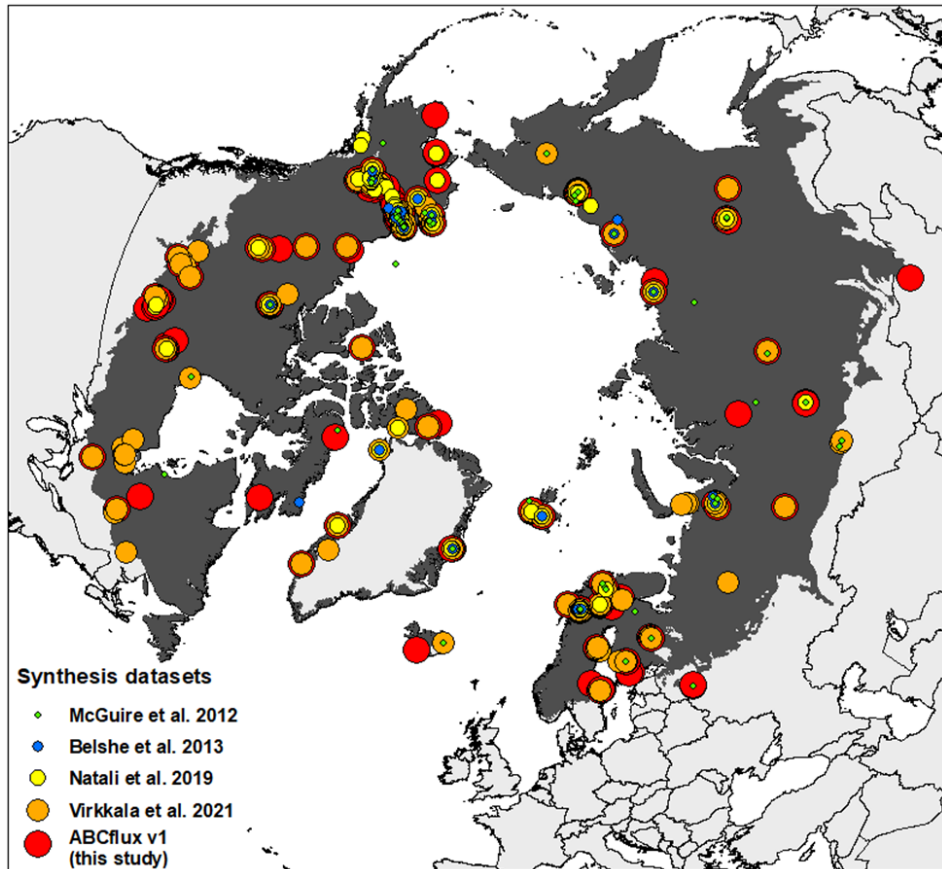


Fig 1. The flux site distribution in previous syntheses that focused on compiling fluxes from high latitudes (McGuire et al. 2012, Belshe et al. 2013, Natali et al. [2019](#)[2019a](#), Virkkala et al. 2021b and this study (ABCflux)). The Arctic-Boreal Zone is highlighted in dark grey; countries are shown in the background. Based on the unique latitude-longitude coordinate combinations in the tundra, there were 136 tundra sites in ABCflux, 104 tundra sites in Virkkala et al. 2021b, 68 tundra sites in Natali et al., [2019](#)[2019a](#), 34 tundra sites in Belshe et al. 2013, and 66 tundra sites in McGuire et al.,

2012. Observations that were included in previous studies but not in ABCflux represent fluxes aggregated over seasonal, not monthly periods.

**Table 1. A summary of past CO<sub>2</sub> flux synthesis efforts. If site numbers were not provided in the paper, this was calculated as the number of unique sets of coordinates.**

Study	Number of sites	Synthesized fluxes and measurement techniques	Study domain	Study period	Flux aggregation
Luyssaert et al. (2007)	NA	GPP, Reco, and NEE measured with eddy covariance	Global forests (including boreal)	NA	Annual
McGuire et al. (2012)	<del>6066</del>	GPP, Reco, and NEE measured with chambers, eddy covariance, diffusion technique and soda lime	Arctic tundra	Measurements from 1966-2009; focus on 1990-2009	Annual, growing and winter season
Belshe et al. (2013)	34	GPP, Reco, and NEE measured with chambers, eddy covariance, diffusion technique and soda lime	Arctic tundra	Measurements from 1966-2010	Annual, growing and winter season
Baldocchi et al. (2018)	9	GPP, Reco, and NEE measured with eddy covariance	Global (including boreal and tundra biomes)	NA (sites with 5-18 years of measurements)	Annual

Virkkala et al. (2018)	117	GPP, Reco, and NEE measured with chambers	Arctic tundra	Studies published during 2000-2016	Growing season
Natali et al. (2019, 2019a)	104	Soil respiration <del>(of NEE)</del> and NEE measured with chambers, eddy covariance, diffusion technique, and soda lime	Northern permafrost region	Measurements from 1989-2017, focus on 2000-2017	Monthly or seasonal during winter
Virkkala et al. (2021b)	148	GPP, Reco, and NEE measured with chambers and eddy covariance	Arctic tundra and boreal biomes	1990-2015	Annual and growing season
ABCflux version 1 (this study)	244	GPP, Reco, and NEE (with some soil respiration and forest floor fluxes) measured with chambers, eddy covariance, and diffusion technique	Arctic tundra and boreal biomes	1989-2020	Monthly (whole year)

## 2. Data and methods

ABCflux focuses on the area covered by the northern tundra and boreal biomes ( $>45^{\circ}\text{N}$ ), as characterized in (Dinerstein et al., 2017, Fig. 2)), and compiles *in-situ* measured terrestrial ecosystem-level  $\text{CO}_2$  fluxes aggregated to monthly time periods (unit:  $\text{g C m}^{-2} \text{ month}^{-1}$ ). We chose this aggregation interval as monthly temporal frequency is a common, straightforward, and standard interval used in many synthesis, modeling studies, remote sensing products, and process model output (Didan, 2015; Natali et al., 2019a; Hayes et al., 2014). Furthermore, scientific

papers often report monthly fluxes, facilitating accurate extraction to ABCflux. We compiled only aggregated fluxes to allow easy usage of the database, and to keep the database concise and cohesive. We designed this database so that these monthly fluxes, compiled from scientific papers or data repositories or contributed by site principal investigators (PIs), can be explored from as many sites as possible and across different months, regions and ecosystems. The database is not designed for studies exploring flux variability within a month, or how different methodological decisions (e.g., flux filtering or partitioning approaches) influence the estimated fluxes. If a potential data user requires fluxes at higher temporal frequency or is interested to study the uncertainties related to flux processing, we suggest they utilize data from other flux repositories (see Section 2.1.2.) or contact PIs.

Although the three flux measurement techniques included in ABCflux primarily measure NEE, chamber and eddy covariance techniques can also be used to estimate GPP (the photosynthetic flux) and Reco (comprising emissions from autotrophic and heterotrophic respiration) (Keenan and Williams, 2018), which are also included in the database. At eddy covariance sites, GPP and Reco are indirectly derived from NEE using partitioning methods that primarily use light and temperature data (Lasslop et al., 2010; Reichstein et al., 2005). At chamber sites, Reco can be measured directly with dark chambers, from which GPP can be calculated by subtracting Reco from NEE (Shaver et al., 2007). In general, these partitioned GPP and Reco fluxes have higher uncertainties than the NEE measurements since they are modeled based on additional data and various assumptions (Aubinet et al., 2012). However, GPP and Reco fluxes were included in ABCflux because these component fluxes may help to better understand and quantify the underlying processes of land–atmosphere CO<sub>2</sub> exchange.

In addition to CO<sub>2</sub> fluxes, we gathered information describing the general site conditions (e.g., site name, coordinates, vegetation type, disturbance history, a categorical soil moisture variable, and soil organic carbon stocks), micrometeorological and environmental measurements (e.g., air and soil temperatures, precipitation, soil moisture, snow depth), and flux measurement technique

(e.g., measurement frequency, instrumentation, gap-filling and partitioning method, number of spatial replicates for chamber measurements, flux data quality), wherever possible.

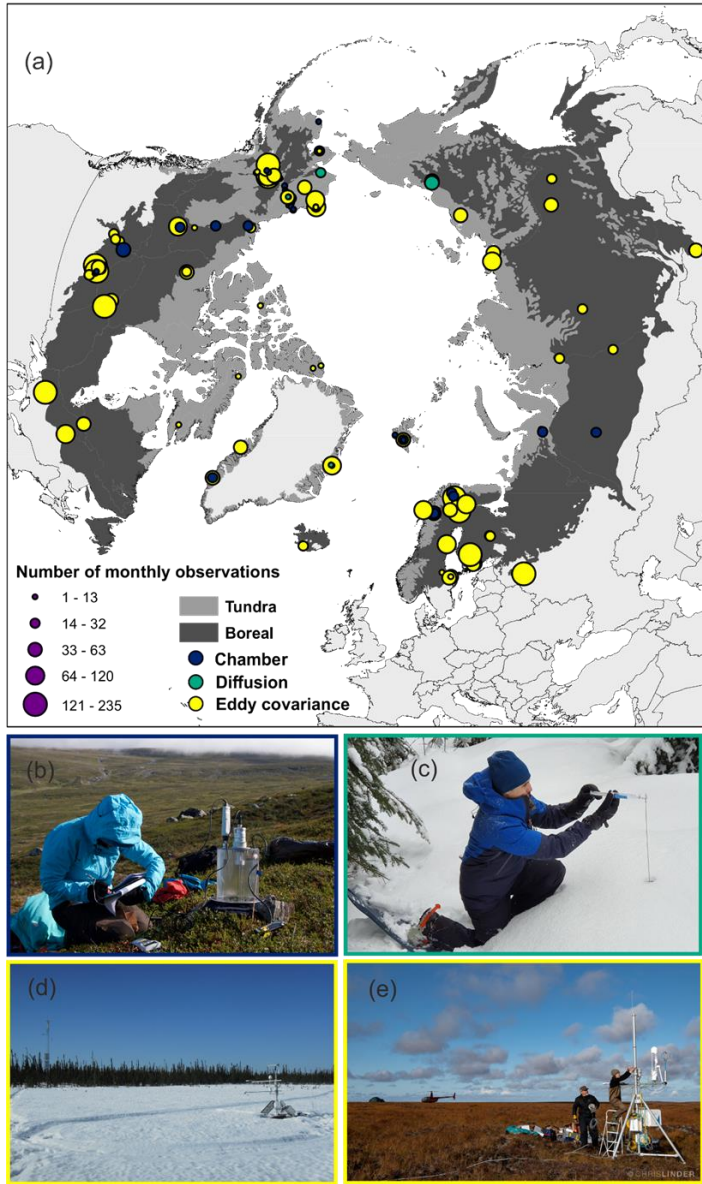


Fig 2. Map showing the distribution and measurement technique at each site (a), and examples of ~~an eddy covariance tower (b)~~, a manual chamber (c), diffusion measurements (d), and two eddy



covariance towers in ~~wetland and forest (e). Photographs were taken in Yukon-Kuskokwim Delta, Alaska (September 2019),~~ a wetland-forest and tundra ecosystem (d-e). Photographs were taken in Kilpisjärvi, Finland (July 2016), Montmorency forest, Canada (April 2021), and Scotty Creek, Canada (April, 2014), and Yukon-Kuskokwim Delta, Alaska (September 2019). Image credits to: Markus Jylhä, Alex Mavrovic, Gabriel Hould Gosselin, Chris Linder, Manuel Helbig.

## 2.1. Data sources

### 2.1.1 Literature search

We identified potential CO<sub>2</sub> flux studies and sites from prior synthesis efforts (Belshe et al., 2013; McGuire et al., 2012; Virkkala et al., 2018; Natali et al., ~~2019~~2019a; Virkkala et al., 2021b), including a search of citations within and of the studies included in these prior syntheses. We also conducted a literature search with the search words (“carbon flux” or “carbon dioxide flux” or “NEE” or “net ecosystem exchange”), and (“arctic” or “tundra” or “boreal”) in Web of Science to ensure that our database included the most recent publications. We included studies that reported at least NEE, presented at monthly or finer temporal resolution, and had supporting environmental ancillary data describing the sites. We ~~extracted our variables of interest (Section 2.3.) from these selected papers during 2018–2020. Data from line and bar plots were extracted using Plot Digitizer (<http://plotdigitizer.sourceforge.net/>) and converted to our flux units (g C m<sup>-2</sup> month<sup>-1</sup>) if needed. Papers including a low number of temporal replicates within a month (<3 individual measurements in summer months) and only one measurement month were disregarded. For the spring (March–May), autumn (September–November), and winter (December–February) months, one temporal replicate was accepted due to scarcity of measurements outside the summer season (June–August); measurement frequency is included in the database. Data from experimental treatments were excluded; however, we included flux data from unmanipulated control plots~~ did not include fluxes reported at longer timesteps (e.g., seasonal aggregations), which, based on our rough estimate, resulted in a 10–20 % loss of data from sites and periods that would have been new to ABCflux. These excluded data primarily included some older, non-active eddy covariance sites and seasonal chamber measurements (e.g., (Nobrega and Grogan, 2008; Heliasz et al., 2011; Fox et al., 2008)). However, many of these

data were located in the vicinity of existing sites covered by ABCflux (e.g., Daring Lake, Abisko), thus excluding these measurements does not dramatically influence the geographical coverage of the sites. We extracted our variables of interest (Section 2.3.) from these selected papers during 2018-2020. Data from line and bar plots were extracted using Plot Digitizer (<http://plotdigitizer.sourceforge.net/>) and converted to our flux units ( $\text{g C m}^{-2} \text{ month}^{-1}$ ) if needed. Data from experimental treatments were excluded; however, we included flux data from unmanipulated control plots. Monthly non-growing season fluxes from Natali et al., (2019a) were extracted from the recently published data compilation (Natali et al., 2019b). Winter chamber or diffusion measurements in forests from Natali et al., (2019,2019b) were included in the “Ground\_NEEground\_nee” field, which represents forest understory (not whole-ecosystem) NEE.

### **2.1.2. Flux repositories**

We downloaded eddy covariance and supporting environmental data products from AmeriFlux (Novick et al., 2018), Fluxnet2015 (Pastorello et al., 2020), EuroFlux database cluster (ICOS, Carbon Extreme, Carbo Africa, GHG Europe, Carbo Italy, INGOS) (Paris et al., 2012; Valentini, 2003), and Station for Measuring Ecosystem-Atmosphere Relations (Hari et al., 2013). ~~Data were downloaded in 2018-2020. When only daily gap-filled data were supplied, we summed the data to monthly time steps and recorded the percentage of gap-filled data. We did not aggregate any repository GPP, Reco, or NEE datasets that were not gap-filled. We filtered out measurements with low turbulence conditions based on friction velocity (USTAR) thresholds (Aubinet et al., 2012) that were filtered for USTAR (i.e., low friction velocity conditions) and gap-filled were downloaded from repositories in 2018-2020.~~ USTAR varied among sites due to differing site-level assumptions. We downloaded only gap-filled data that met the USTAR criteria for either the tower PI or given through the database processing pipeline. However, Fluxnet2015 provides several different methods for determining data quality based on different USTAR criteria. In this case, we used the Fluxnet2015 common USTAR threshold (CUT, i.e. all years at the site filtered with the same USTAR threshold (Pastorello et al., 2020)). For observations extracted from EuroFlux, USTAR thresholds for each site were derived as

described in (Papale et al., 2006; Reichstein et al., 2005) using night-time data. We extracted fluxes readily aggregated to monthly intervals by the data processing pipeline from Fluxnet2015 and EuroFlux. These aggregations were not given in AmeriFlux and SMEAR. We downloaded daily gap-filled data from these repositories and summed the data to monthly time steps. We did not aggregate any repository GPP, Reco, or NEE datasets that were not gap-filled. If fluxes were available for the same site and period both in Natali et al., (20192019b) and flux repository extractions, the flux repository observations were kept in the database. Some repositories supplied eddy covariance data version numbers, which were added to the flux database.

### **2.1.3. Permafrost Carbon Network data solicitation**

A community call was solicited in 2018 through a CO<sub>2</sub> flux synthesis workshop (Parmentier et al., 2019, Reconciling historical and contemporary trends in terrestrial carbon exchange of the northern permafrost-zone, 2021), whereby the network of ABZ flux researchers were contacted and invited to contribute their most current unpublished eddy covariance and chamber data. This resulted in an additional 39 sites and 1372 monthly observations (see column Extraction\_sourceextraction\_source).

## **2.2. Partitioning approaches at eddy covariance flux sites**

ABCflux compiles eddy covariance observations that were primarily partitioned using night-time Reco, which is based on the assumption that during night, NEE measured at low light levels is equivalent to Reco (Reichstein et al., 2005). This night-time partitioning approach has been the most frequently used approach to fill gaps in flux time series (Wutzler et al., 2018) due to its simplicity, strong evidence of temperature sensitivity of respiration, and direct use of Reco (i.e. night-time NEE) flux data to estimate temperature response curves (Reichstein et al., 2005). As the night-time approach was one of the first widely used partitioning approaches, fluxes partitioned with the approach were the only ones available in the flux repositories at some of the older sites. Daytime partitioning and other approaches started to develop more rapidly in the 2010s (Lasslop et al., 2010; Tramontana et al., 2020). Each of the partitioning approaches have

uncertainties related to the ecological assumptions, input data, model parameters, and statistical approaches used to fill the gaps.

PIs that submitted data to us directly gap-filled and partitioned fluxes using the approach that they determined works best at their site. Based on similar logic, fluxes extracted from papers were not always partitioned using the night-time approach. In these cases, we trusted the expertise of PIs and authors, and included fluxes partitioned using other methods. Although this created some heterogeneity in the flux processing algorithms in the database, this approach was chosen so that we could be more inclusive with the represented sites.

Thus, in summary, our goal was to compile fluxes that 1) can be easily compared with each other (i.e., have been gap-filled and partitioned in a systematic way), 2) are as accurate as possible given the site conditions and measurement setup (i.e., other approaches were accepted if this was suggested by the PI), and 3) summarize information about the processing algorithms used.

### **2.3. Data quality screening**

We screened for poor-quality data, potential unit and sign convention issues, and inaccurate coordinates. Repository eddy covariance data were processed and quality checked using quality flags associated with monthly data supplied by the repository processing pipeline. Fluxnet2015 and EuroFlux database include an aggregated data quality flag (fraction between 0-1, indicating percentage of measured and good-quality gap-filled data for the monthly aggregated data indicating percentage of measured (quality flag QC = 0 in FLUXNET2015) and good-quality gap-filled data (quality flag QC = 1 in FLUXNET2015; average from ~~daily~~monthly data; 0=extensive gap-filling, 1=low gap-filling); for more details see- (Pastorello et al., 2020)) which is reported for fluxes aggregated from finer temporal resolutions Fluxnet2015 web page (<https://fluxnet.org/data/fluxnet2015-dataset/variables-quick-start-guide/>) and (Pastorello et al., 2020)). Note that this quality flag field for the aggregated data differs from the ones calculated

for half-hourly data derived directly from eddy covariance tower processing programs (such as Eddypro). We removed monthly data with a quality flag of 0. Eddy covariance dataData with quality flags >0 were left within the database for the user to decide on additional screening criteria. The database also includes a column describing the percentage of gap-filled data (0=no gap-filled data, 100=completely gap-filled data), however it was not used in data quality screening. TheseNote that the monthly data produced by the repository processing pipeline do not include separate gap-filled percentages or errors of model fit for NEE similar to those associated with the half-hourly data. However, we included these fields to the database as PIs contributing data or scientific papers sometimes had this information; however these fields were not used in data quality screening. Both the monthly quality flag and gap-filled percentage fields describe the amount and quality of the gap-filled data that ~~need~~needed to be filled due to, for example, instrument malfunction, power shortage, extreme weather events, and periods with insufficient turbulence conditions.

At chamber and diffusion sites, we disregarded observations including a low number of temporal replicates within a month (<3 individual measurements in summer months) and only one measurement month to ensure the temporal representativeness of the measurements. For the spring (March-May), autumn (September-November), and winter (December-February) months, one temporal replicate was accepted due to scarcity of measurements outside the summer season (June-August); measurement frequency is included in the database. We excluded monthly summertime measurements with <3 temporal replicates because within summer months, meteorological conditions and the phenological status of the ecosystem can vary significantly (Lafleur et al., 2012; Euskirchen et al., 2012; Schneider et al., 2012; Heiskanen et al., 2021), and a single measurement is unlikely to capture this variability. Our decision to exclude measurements that have only one measurement month was based on our goal to assess the temporal variability of fluxes. We justified the acceptance of a lower number of temporal replicates for the other seasons based on the assumption that flux variability is lower during the winter months, and at least during most of the spring and autumn months, due to the insulating effects of snow (Aurela et al., 2002; Bäckstrand et al., 2010). We estimate that excluding measurements with <3 temporal replicates during the summer months resulted in a 10 % loss of

data. In total, 98 % of the chamber observations were from published studies; we assume that the peer review process assessed the quality of published data.

We further screened for spatial coordinate accuracy by visualizing the sites on a map. If a given site was located in water or had imprecise coordinates, the site researchers were contacted for more precise coordinates. We screened for potential duplicate sites and observations that were extracted from different data sources. Duplicate NEE extracted from papers that were also extracted from flux repositories were compared to estimate uncertainties associated with paper extractions using Plot Digitizer as a means for extracting monthly fluxes. A linear regression between paper (Plot Digitizer) and repository extraction showed that data extracted using Plot Digitizer were highly correlated with data from online databases, providing confidence in estimates extracted using Plot Digitizer ( $R^2=0.91$ , slope = 1.002,  $n=192$ ). Out of these duplicate observations, we only kept the data extracted from the repository in the database. Finally, we asked site principal investigators (PIs)PIs to verify that the resulting information was correct.

#### **2.32.4. Database structure and columns**

The resulting ABCflux database includes 94 variables: 16 are flux measurements and associated metadata (e.g., NEE, measurement date and duration), 21 describe flux measurement methods (e.g., measurement frequency, gap-filling method), 49 describe site conditions (e.g., soil moisture, air temperature, vegetation type), and 8 describe the extraction source (e.g., primary author or site PI, citation, data maturity). 61 variables are considered static and thus do not vary with repeated measurements at a site (e.g., site name, coordinates, vegetation type), while 33 variables are considered dynamic and vary monthly (e.g., soil temperature). Table 2 includes a description of each of the 94 variables, as well as the proportion of monthly observations present in each column. ABCflux is shared as a comma separated values (csv) file with 6309 rows; however, not all the rows have data in each column (indicated by NA for character columns and -9999 for numeric columns).

We refer to all fields included in ABCflux as ~~observations~~“observations” although we acknowledge that, for example, GPP and Reco are indirectly derived variables at eddy covariance sites, and that some flux and ancillary data can also be partly gap-filled. Further, our database does not include the actual raw observations, rather it provides monthly aggregates. Positive values for NEE indicate net CO<sub>2</sub> loss to the atmosphere (i.e., CO<sub>2</sub> source) and negative numbers indicate net CO<sub>2</sub> uptake by the ecosystem (i.e., CO<sub>2</sub> sink). For consistency, GPP is presented as negative (uptake) values and Reco as positive.

**Table 2. Database variables and the proportion of monthly observations in each variable. There are in total 6309 monthly observations in the database.**

Variable	Variable description and units	Details	Proportion of monthly observations having data
id	ID given to each individual monthly entry at each site		100%
<del>Study_ID</del> <u>study_id</u>	ID given to study/site entry (see Details)	(PI/first author of publication)_(site name)_(tower/chamber)_(#); Eg., Schuur_EML_Tower_1. Note that there might be several chamber (or tower) Study_IDs for one site.	100%
<del>Study_ID_Short</del> <u>study_id_short</u>	ID given to study/site entry (see Details), individual chamber plots within a site not differentiated	(PI/first author of publication)_(site name)_(tower/chamber)_(#); Eg., Schuur_EML_Tower_1.	100%

<u>Site_Name</u> <u>site_name</u>	Site name as specified in data source	Usually the location name	100%
<u>Site_Reference</u> <u>site_reference</u>	A more specific name used in data source	For towers, this is often the acronym for the site, and for chambers, this is the name of the particular chamber plot	95%
<u>Data_contributor_or_Author</u> <u>country</u>	<u>Data contributor(s) or primary author(s) associated with data set or publication</u> <u>Country of the site</u>	<u>If you use unpublished data or data from flux repositories (see Extraction_source), please contact this person</u>	100%
<u>Latitude</u> <u>latitude</u>	Decimal degrees, as precise as possible		100%
<u>Longitude</u> <u>longitude</u>	Decimal degrees, as precise as possible	Negative longitudes are west from Greenwich	100%
<u>Email</u> <u>start_date</u>	<u>Primary author email</u> <u>Date on which measurement starts</u>	<u>-mm/dd/yyyy</u>	<u>93</u> 100%
<u>ORCID</u> <u>end_date</u>	<u>personal digital identifier: https://orcid.org/</u> <u>Date on which measurement ends</u>	<u>-mm/dd/yyyy</u>	<u>29</u> 100%
<u>Citation</u> <u>meas_year</u>	<u>Journal article, data citation, and/or other source (online repository, PI submitted, etc.)</u> <u>Year in which data were recorded</u>		<u>70</u> 100%

Formatted Table



<u>Data_adderseason</u>	The person(s) who added the data to the database <u>Season in which data were recorded</u>	Primarily researchers working at Woodwell <u>summer, autumn, winter, spring</u> (based on climatological seasons)	100%
<u>Data_availabilityinterval_month</u>	Current availability of data: data available in a published paper, in an open online data repository, in an already published synthesis, or user contributed <u>Measurement month</u>	Published_Paper, Published_Online, Published_Synthesis, User_Contributed	100%
<u>Data_maturitystart_day</u>	Current maturity of data <u>Start day of the measurement</u>	Preliminary, Processed, Published, Reprocessed	100%
<u>Extraction_sourceend_day</u>	Data source <u>End day of the measurement</u>	paper, Virkkala or Natali syntheses, Euroflux, Fluxnet-2015, PI, Ameriflux, SMEAR, ORNL DAAC, Pangaea	100%
<u>Biomeuration</u>	Biome <u>Number of the site days during the measurement month</u>	Boreal, Tundra <u>Should be the same as End_Day because this database compiles monthly fluxes</u>	100%
<u>Veg_typebiome</u>	A detailed vegetation type for <u>Biome of the site</u>	B1=cryptogam, herb barren; B2=cryptogam barren complex; B3=noncarbonate mountain complex; B4=carbonate mountain complex; G1=rush/grass, forb, cryptogam tundra; G2=graminoid, prostrate dwarf shrub, forb tundra; G3=nontussock sedge, dwarf shrub, moss tundra; G4=tussock sedge, dwarf shrub, herb tundra; P1=prostrate dwarf shrub, herb tundra; P2=prostrate/hemiprostrate dwarf shrub tundra; S1=erect dwarf shrub tundra; S2=low shrub tundra; W1=sedge/grass, moss wetland; W2=sedge, moss, dwarf shrub wetland; W3=sedge, moss, low shrub wetland; DB=deciduous broadleaf forest; EN=evergreen needleleaf forest; DN=deciduous needleleaf forest; MF=mixed forest; SB=sparse boreal vegetation; BW=boreal wetland or peatland, following Watts et al. (2019). For more details about	100%

		<p>the tundra vegetation types; see Walker et al. (2005). These classes were classified based on information in Site_Reference and Veg_detail columns, or were contributed by the site PI-Boreal_Tundra</p>	
Veg_type_Shortveg_type	A more general detailed vegetation type for the site	<p>B=barren B1=cryptogram, herb barren; B2=cryptogram barren complex; B3=noncarbonate mountain complex; B4=carbonate mountain complex; G1=rush/grass, forb, cryptogram tundra; G2=graminoid tundra; P=prostrate dwarf-shrub, forb tundra; G3=tussock sedge, dwarf-shrub, moss tundra; G4=tussock-sedge, dwarf-shrub, herb tundra; P1=prostrate dwarf-shrub, herb tundra; S=shrub tundra; W=tundra P2=prostrate/hemiprostrate dwarf-shrub tundra; S1=erect dwarf-shrub tundra; S2=low-shrub tundra; W1=sedge/grass, moss wetland; W2=sedge, moss, dwarf-shrub wetland; W3=sedge, moss, low-shrub wetland; DB=deciduous broadleaf forest; EN=evergreen needleleaf forest; DN=deciduous needleleaf forest; MF=mixed forest; SB=sparse boreal vegetation; BW=boreal wetland or peatland, following Watts et al. (2019). For more details about the tundra vegetation types, see Walker et al. (2005). These classes were classified based on information in Site_Reference and Veg_detail columns, or were contributed by the site PI.</p>	100%
Veg_detailveg_type_short	Detailed vegetation description from data source/contributor; A more general vegetation type for the site	<p>B=barren tundra; G=graminoid tundra; P=prostrate dwarf-shrub tundra; S=shrub tundra; W=tundra wetland; DB=deciduous broadleaf forest; EN=evergreen needleleaf forest; DN=deciduous needleleaf forest; MF=mixed forest; SB=sparse boreal vegetation; BW=boreal wetland or peatland. For more details about the tundra vegetation types, see Walker et al. (2005). These classes were classified based on information in Site_Reference and Veg_detail columns, or were contributed by the site PI.</p>	96100%

<a href="#">Countryveg_detail</a>	<a href="#">Country-of-the-siteDetailed vegetation description from data source/contributor</a>		10096%
<a href="#">Permafrostpermafrost</a>	Reported presence or absence of permafrost	Yes, No	7273%
<a href="#">Disturbancedisturbance</a>	Last disturbance	Fire, Harvest, Thermokarst, Drainage, Grazing, Larval Outbreak, Drought	30%
<a href="#">Disturb_yeardisturb_year</a>	Year of last disturbance	Numeric variable, 0 = annual (e.g., annual grazing)	23%
<a href="#">Disturb_severitydisturb_severity</a>	Relative severity of disturbance	High, Low	11%
<a href="#">Soil_moisture_classsoil_moisture_class</a>	General descriptor of site moisture	Wet = At least sometimes inundated or water table close to surface. Dry = well-drained.	56%
<a href="#">Site_activitysite_activity</a>	Describes whether the site is currently active (i.e., measurements conducted each year)	Yes, No. Eddy covariance information was extracted from <a href="https://cosima.nceas.ucsb.edu/carbon-flux-sites/">https://cosima.nceas.ucsb.edu/carbon-flux-sites/</a> by assuming that sites that were active in 2017 are still continuing to be active. We used our expertise to define active chamber sites that have measurements at least during each growing season.	60%
<a href="#">Meas_yearnee</a>	<a href="#">Year in which data were recordedNet Ecosystem Exchange (g C-CO<sub>2</sub>m<sup>-2</sup> for the entire measurement interval)</a>	<a href="#">-Convention: -ve is uptake, +ve is loss.</a>	10091%
<a href="#">Seasongpp</a>	<a href="#">Season in which data were recordedGross Primary Productivity (g C-CO<sub>2</sub>m<sup>-2</sup> for</a>	<a href="#">summer, autumn, winter, spring (based on climatological seasons)Report as -ve flux</a>	10068%

	<u>the entire measurement interval)</u>		
<u>Interval</u> <u>reco</u>	<u>Measurement-monthEcosystem Respiration (g C-CO<sub>2</sub> m<sup>-2</sup> for the entire measurement interval)</u>	<u>-Report as +ve flux</u>	<u>+0073%</u>
<u>Start_day</u> <u>ground_nee</u>	<u>Start-day-of-the measurementForest floor Net Ecosystem Exchange, measured with chambers (g C-CO<sub>2</sub> m<sup>-2</sup> for the entire measurement interval)</u>	<u>-Convention: -ve is uptake, +ve is loss. Chamber measurements from (primarily rather treeless) wetlands are included in the NEE_gC_m2 column.</u>	<u>+004%</u>
<u>End_day</u> <u>ground_gpp</u>	<u>End-day-of-the measurementForest floor Ecosystem Respiration, measured with chambers (g C-CO<sub>2</sub> m<sup>-2</sup> for the entire measurement interval)</u>	<u>-Report as -ve flux. Chamber measurements from (primarily rather treeless) wetlands are included in the GPP_gC_m2 column.</u>	<u>+001%</u>
<u>Duration</u> <u>ground_reco</u>	<u>Number-of-days-during-the measurement-monthForest floor Gross Primary Productivity, measured with chambers (g C-CO<sub>2</sub> m<sup>-2</sup> for the entire measurement interval)</u>	<u>Should-be-the-same-as-End_Day-because-this database-compiles-monthly-fluxes. Report as +ve flux. Chamber measurements from (primarily rather treeless) wetlands are included in the Reco_gC_m2 column.</u>	<u>+002%</u>
<u>Start_date</u> <u>soil</u>	<u>Date-on-which-measurement startsSoil respiration, measured with chambers (g C-CO<sub>2</sub> m<sup>-2</sup> for the entire measurement interval)</u>	<u>dd/mm/yyyyReport as +ve flux</u>	<u>+004%</u>

<a href="#">End_dateflux_method</a>	Date on which measurement ends How flux values were measured	dd/mm/yyyy EC=eddy covariance, Ch=chamber, Diff=diffusion methods. No observations from experimental manipulation plots	100%
<a href="#">NEE_gC_m2flux_method_detail</a>	Net Ecosystem Exchange (g C-CO <sub>2</sub> m <sup>-2</sup> for the entire measurement interval) Details related to how flux values were measured: closed- and open-path eddy covariance, mostly manual chamber measurements, mostly automated chamber measurements, a combination of chamber and cuvette measurements, diffusion measurements through the snowpack, chamber measurements on top of snow	Convention: -ve is uptake, +ve is loss. EC_closed, EC_open, EC_enclosed, EC_open & closed, EC_enclosed, Chambers_manual, Chambers_automated, Chambers_CUV, Snow_diffusion, Chambers_snow, NA	94.93%
<a href="#">GPP_gC_m2measurement_frequency</a>	Gross Primary Productivity (g C-CO <sub>2</sub> m <sup>-2</sup> for the entire measurement interval) Frequency of flux measurements	Report as -ve flux > 100 characterizes high-frequency eddy covariance (and automated chamber) measurements. Manual chamber and diffusion techniques often have values between 1 and 30; 1=measurements done during one day of the month, 30=measurements done daily throughout the month. This is the primary variable that characterizes the frequency and gaps in monthly fluxes estimated with chambers and diffusion techniques.	68.100%
<a href="#">Reco_gC_m2diurnal_coverage</a>	Ecosystem Respiration (g C-CO <sub>2</sub> m <sup>-2</sup> for the entire measurement interval) Times of day covered by flux measurements	Report as +ve flux Day, Day and Night	73.90%
<a href="#">Ground_NEE_gC_m2partition_method</a>	Forest floor Net Ecosystem Exchange, measured with chambers (g C-CO <sub>2</sub> m <sup>-2</sup> for the	Convention: -ve is uptake, +ve is loss. Chamber measurements from (primarily rather treeless) wetlands are included in the NEE_gC_m2	4.16%

	entire measurement interval) Method used to partition NEE into GPP and Reco	column-Reichstein (night time=Reco partitioning), Lasslop (bulk/day-time partitioning), Reco_measured, ANN, or GPP=Reco-NEE (for chamber sites)	
Ground_GPP_gC_m2spatial_reps_chamber	Forest floor-Ecosystem Respiration, measured with chambers (g C-CO <sub>2</sub> -m <sup>-2</sup> for the entire measurement interval) Number of spatial replicates for the chamber plot	Report as -ve flux. Chamber measurements from (primarily rather treeless) wetlands are included in the GPP_gC_m2 column. Usually, but not always, several chamber plots are measured to assure the representativeness of measurements	47%
Ground_Reco_gC_m2gap_fill	Forest floor-Gross Primary Productivity, measured with chambers (g C-CO <sub>2</sub> -m <sup>-2</sup> for the entire measurement interval) Gap filling method	Report as +ve flux. Chamber measurements from (primarily rather treeless) wetlands are included in the Reco_gC_m2 column-e.g., Average, Linear interpolation, Lookup table, MDS (marginal distribution sampling), Light/temperature response, Neural network, a combination of these, or a longer description related to chamber measurements	270%
Rsoil_gC_m2gap_perc	Soil respiration, measured with chambers (g C-CO <sub>2</sub> -m <sup>-2</sup> for the entire measurement interval) % of NEE data that was gap-filled in the measurement interval (relative to standard measurement time step)	Report as +ve flux. Reported mainly for eddy covariance data	417%
Flux_methodtower_qa_qc_nee_flag	How flux values were measured Overall monthly quality flag for eddy covariance aggregated observations; fraction between 0-1, indicating percentage of measured and good-quality gap-filled data	EC=eddy covariance, Ch=chamber, Diff=diffusion methods. No observations from experimental manipulation plots 0=extensive gap-filling, 1=low gap-filling	1004%

<a href="#">Flux_method_detailtower_qa_qc_nee_source</a>	Details related to how flux values were measured: closed- and open-path eddy covariance; mostly manual-chamber measurements, mostly automated-chamber measurements, a combination of chamber and cuvette measurements, diffusion measurements through the snowpack, chamber measurements on top of snow The source for the overall quality information for the eddy covariance observations	EC_closed, EC_open, EC_enclosed, EC_open & closed, EC_enclosed, Chambers_mostly_manual, Chambers_mostly_automatic, Chambers_CUV, Snow_diffusion, Chambers_snow, NA0=Fluxnet2015, 1=Euroflux	9337%
<a href="#">Measurement_frequency_method_error_nee</a>	Frequency of flux measurements RMSE or other bootstrapped error of model fit for NEE (g C-CO <sub>2</sub> m <sup>-2</sup> for the entire measurement interval)	>100 characterizes high-frequency measurements. Manual-chamber and diffusion techniques often have values between 1 and 30; 1=measurements done during one day of the month, 30=measurements done daily throughout the month.	10023%
<a href="#">Diurnal_coverage_method_error_technique</a>	Times of day covered by Technique used to quantify method errors for flux measurements	Day, Day and Nighte.g., gap-filling and partitioning errors or uncertainty in data-model fit: bootstrap, MCMC, RMSE fit, etc.	901%
<a href="#">Partition_method_high_freq_availability</a>	Method used to partition NEE into GPP and Reco Availability of high-frequency data	Reichstein (night-time-Reco partitioning); Lasslop (bulk/day-time partitioning); Reco_measured; ANN; or GPP=Reco-NEE (for chamber sites)	1617%
<a href="#">Spatial_reps_chamber_aggregation_method</a>	Number of spatial replicates for the chamber plot Method used to aggregate data to measurement interval	Usually, but not always, several chamber plots are measured to assure the representativeness of measurements	7158%

<a href="#">Gap_fillinstrumentation</a>	Gap filling method>Description of instrumentation used	e.g., Average, Linear interpolation, Lookup table, MDS (marginal distribution sampling); Light/temperature response, Neural network, a combination of these, or a longer description related to chamber measurements	7068%
<a href="#">Gap_peretower_Version</a>	% of NEE data that was gap-filled in the measurement interval (relative to standard measurement time step)Version number of the eddy covariance dataset from the extraction source		4721%
<a href="#">Tower_QA.QC.NEE.flags_tower_data_restriction</a>	Overall monthly quality flag for eddy covariance aggregated observations; fraction between 0-1, indicating percentage of measured and good-quality gap-filled data	0=extensive gap-filling, 1=low gap-filling	4412%
<a href="#">QA.QC.source_tower_corrections</a>	The source for the overall quality information for the eddy covariance observationsDetails related to processing corrections employed, including time, duration, and thresholds for u* and heat corrections	0=Fluxnet2015, 1=Euroflux	3732%
<a href="#">Precip_int_mm_spatial_variation_technique</a>	Total precipitation during measurement interval (mm)Technique used to quantify spatial variation for flux measurements	e.g., standard error of replicate measurements for chambers, spatial error based on footprint partitioning for towers	3710%



<a href="#">Tair_int_Clight_response_method_chamber</a>	Mean air temperature during measurement interval (°C) <a href="#">Details related to how the varying light response conditions were considered in chamber measurements</a>		725%
<a href="#">Tsoil_Cpar_cutoff</a>	Mean soil Temperature during measurement interval (°C) <a href="#">PAR level used to define night-time data and apply partitioning method (umol PAR m<sup>-2</sup> second<sup>-1</sup>)</a>		7417%
<a href="#">Soil_moisture_pereprecip_int</a>	Mean soil moisture <a href="#">Total precipitation during the measurement interval (% by volume)</a>		3537%
<a href="#">Thaw_depth_emair_int</a>	Mean thaw depth <a href="#">air temperature during the measurement interval (em°C)</a>	Report with positive values	672%
<a href="#">Tsoil_depth_emsoil</a>	Depth of soil temperature measurement below surface <a href="#">(emMean soil Temperature during measurement interval (°C))</a>		4674%
<a href="#">Moisture_depth_emsoil_moisture</a>	Depth of <a href="#">Mean soil moisture measurement below surface (emduring the measurement interval (% by volume))</a>		3135%
<a href="#">ALT_emthaw_depth</a>	Active layer thickness (em; maximum thaw depth); will	Report with positive values	156%

Formatted Table

Formatted Table

	<u>change annually</u> Mean thaw depth during the measurement interval (cm)		
<u>WTD_cmsoil_depth</u>	Mean water table depth during the measurement interval (cm); Positive is below the surface, negative is aboveDepth of soil temperature measurement below surface (inundatedcm)		746%
<u>Snow_depth_cm</u> moisture_depth	Mean snow depth during the measurement intervalDepth of soil moisture measurement below surface (cm)		1431%
<u>VPD_Paalt</u>	Mean vapour pressure deficit during the measurement interval (Pa)Active layer thickness (cm; maximum thaw depth), will change annually	Report with positive values	3015%
<u>ET_mm</u> water table_depth	Total evapotranspirationMean water table depth during the measurement interval (mmcm); Positive is below the surface, negative is above (inundated)		47%
<u>PAR_W_m2</u> snow_depth	Mean photosynthetically active radiationsnow depth during the measurement interval ( $W \cdot m^{-2} \cdot cm$ )		514%
<u>PAR_PPFD_umol_m2</u> svapor_p ressure_deficit	Mean photosynthetically active radiation during measurement interval (measured in Photosynthetic Photon Flux		1130%

Formatted Table

	<p>Density, PPFD; micromol m<sup>-2</sup> s<sup>-1</sup> vapour pressure deficit during the measurement interval (Pa)</p>		
<p>Precip_ann_mm evapotranspiration</p>	<p>Mean annual precipitation (mm), from site or nearby weather station as a general site descriptor. This should describe the longer term climate for the site rather than a few years of study. Total evapotranspiration during the measurement interval (mm)</p>		80%
<p>Tair_ann_C par</p>	<p>Mean annual air temperature (°C), from site or nearby weather station as a general site descriptor. This should describe the longer term climate for the site rather than a few years of study. photosynthetically active radiation during measurement interval (W m<sup>-2</sup>)</p>		79%
<p>Met_sourcepar_ppfd</p>	<p>Data source and years used to calculate mean annual temperature/precipitation Mean photosynthetically active radiation during measurement interval (measured in Photosynthetic Photon Flux Density, PPFD; micromol m<sup>-2</sup> s<sup>-1</sup>)</p>		50%

<a href="#">Elevation_mprecip_ann</a>	Elevation above sea level (m) Mean annual precipitation (mm), from site or nearby weather station as a general site descriptor. This should describe the longer-term climate for the site rather than a few years of study.		6580%
<a href="#">LAHair_ann</a>	Leaf Area Index Mean annual air temperature (°C), from site or nearby weather station as a general site descriptor. This should describe the longer-term climate for the site rather than a few years of study.		2379%
<a href="#">SOL_depth_emt_precip_source_yrs</a>	Soil organic layer depth (cm) Data source and years used to calculate mean annual temperature/precipitation		2350%
<a href="#">pere_Celevation</a>	Soil carbon percentage (% Elevation above sea level (m))		765%
<a href="#">pere_C_depth_emlai</a>	Depth at which soil carbon % was measured (cm) Leaf Area Index		722%
<a href="#">C_dens_kgC_m2sol_depth</a>	Soil carbon per unit area (kg C m <sup>-2</sup> organic layer depth (cm))		4623%
<a href="#">C_dens_depth_emsoil_perc_carbon</a>	Depth to which Soil organic carbon per unit area was		87%

Formatted Table

	<u>estimated (cmSoil carbon percentage (%)</u>		
<u>AGB_kgC_m2perc_C_depth</u>	<u>Above ground biomass (kg C m<sup>-2</sup>Depth at which soil carbon % was measured (cm)</u>		<u>417%</u>
<u>AGB_typec_density</u>	<u>Types of above ground vegetation included in the AGB measurementSoil carbon per unit area (kg C m<sup>-2</sup>)</u>	<u>Trees, shrubs, graminoids, mosses, lichens</u>	<u>4316%</u>
<u>Soil_typec_density_depth</u>	<u>General soil type, including source (e.g., USDA, CSSC, NCSCDDepth to which soil organic carbon per unit area was estimated (cm)</u>		<u>428%</u>
<u>Soil_type_detailagb</u>	<u>Detailed soil type description, if availableAbove ground biomass (kg C m<sup>-2</sup>)</u>		<u>911%</u>
<u>Citation_Data_Overlapagb_type</u>	<u>Another citation for the siteTypes of above ground vegetation included in the AGB measurement</u>	<u>Trees, shrubs, graminoids, mosses, lichens</u>	<u>13%</u>
<u>High_freq_availabilitysoil_type</u>	<u>Availability of high frequency dataGeneral soil type, including source (e.g., USDA, CSSC, NCSCD)</u>		<u>4742%</u>
<u>Light_response_method_chambe #soil_type_detail</u>	<u>Details related to how the varying light response conditions were considered in</u>		<u>59%</u>

Formatted Table

	<p>chamber measurements Detailed soil type description, if available</p>		
<p>PAR_cutoff_umol_m2_second her_data</p>	<p>PAR level used to define night-time data and apply partitioning method (umol PAR m<sup>-2</sup> second<sup>-1</sup>) Other types of data from the data source that may be relevant</p>		47%
<p>Aggregation_method notes_site_info</p>	<p>Method used to aggregate data to measurement interval Any other relevant information related to static site descriptions</p>		5820%
<p>Instrumentation notes_time_variation</p>	<p>Description of instrumentation used Any other relevant information related to time-varying data</p>		6859%
<p>Tower_Version citation</p>	<p>Version number of the eddy covariance dataset from the extraction source Journal article, data citation, and/or other source (online repository, PI submitted, etc.)</p>		2470%
<p>Spatial_variation_technique citation_data_overlap</p>	<p>Technique used to quantify spatial variation for flux measurements Another citation for the site</p>	<p>e.g., standard error of replicate measurements for chambers, spatial error based on footprint partitioning for towers</p>	4013%

Formatted Table

<a href="#">Method_error_NEE_gC_m2_data_contributor_or_author</a>	RMSE or other bootstrapped error of model fit for NEE (g C-CO <sub>2</sub> m <sup>-2</sup> for the entire measurement interval) Data contributor(s) or primary author(s) associated with data set or publication	-If you use unpublished data or data from flux repositories (see <a href="#">Extraction source</a> ), please contact <a href="#">this person</a>	23/100%
<a href="#">Method_error_technique_email</a>	Technique used to quantify method errors for flux measurements Primary author email	e.g., gap filling and partitioning errors or uncertainty in data model fit: bootstrap, MCMC, RMSE fit, etc.	1/23%
<a href="#">Tower_Data_restriction_orcid</a>	-personal digital identifier: <a href="https://orcid.org/">https://orcid.org/</a>		1/229%
<a href="#">Tower_Corrections_data_availability</a>	Details related to processing corrections employed, including time, duration, and thresholds for u <sup>2</sup> and heat corrections Current availability of data: data available in a published paper, in an open online data repository, in an already published synthesis, or user contributed	-Published Paper, Published Online, Published Synthesis, User Contributed	32/100%
<a href="#">Other_data_data_maturity</a>	Other types Current maturity of data from the data source that may be relevant	-Preliminary, Processed, Published, Reprocessed. Currently, none of the observations belong to the Preliminary or Reprocessed classes, but they were kept for future versions of the database.	7/100%
<a href="#">Notes_Site_Info_extraction_source</a>	Any other relevant information Data source	-paper, Virkkala or Natali syntheses, Euroflux, Fluxnet 2015, PI, Ameriflux, SMEAR, ORNL DAAC, Pangaea	20/100%

Notes_TimeVariant\dataentry_person	Any other relevant information The person(s) who added the data to the database	-Primarily researchers working at Woodwell	59/100%
------------------------------------	--	--	---------

#### 2.4. Database visualization

The visualizations in this paper were made with the full ABCflux database using each site-month as a unique data point (from now on, these are referred to as monthly observations) and the sites listed in the “Study\_ID\_Shortstudy\_id\_short” field. We visualized these across the vegetation types (“Veg\_type\_Shortveg\_type\_short”), countries (“Countrycountry”), biomes (“Biomebiome”), and measurement method (“Flux\_methodflux\_method”).

To understand the distribution and representativeness of monthly observations and sites across the ABCflux as well as the entire ABZ, we used geospatial data to calculate the aerial coverages of each vegetation type and country. Vegetation type was derived from the European Space Agency Climate Change Initiative’s (ESA CCI) land cover product aggregated and resampled to 0.0083° for the boreal biome (Lamarche et al., 2013) and the raster version of the Circumpolar Arctic Vegetation Map (CAVM) for the tundra biome resampled to the same resolution as the ESA CCI product (Raynolds et al., 2019). ESA CCI layers were reclassified by grouping land cover types to the same vegetation type classes represented by ABCflux: boreal wetland and peatland (from now on, boreal wetland; classes 160, 170, 180 in ESA CCI product), deciduous broadleaf forest (60-62), evergreen needleleaf forest (70-72), deciduous needleleaf forest (80-82), mixed forest (90), and sparse and mosaic boreal vegetation (40, 100, 100, 120, 121, 122, 130, 140, 150, 151, 152, 153, 200, 201, 202). Croplands (10, 11, 12, 20, 30) and urban areas (190) were removed. We used the five main physiognomic classes from CAVM in the tundra.



Glaciers and permanent water bodies included in either of these products were removed. Note that in ABCflux and for the site-level visualizations in this paper, vegetation type for each of the flux sites was derived from site-level information, not these geospatial layers. These same glacier, water, and cropland masks were applied to the country boundaries (Natural Earth - Free vector and raster map data at 1:10m, 1:50m, and 1:110m scales, 2021) to calculate the terrestrial area of each country. [We further used TerraClimate annual and seasonal air temperature and precipitation layers averaged over 1989-2020 to visualize the distribution of monthly observations across the Arctic-Boreal climate space \(Abatzoglou et al., 2018\).](#)

### 3. Database summary

#### 3.1. General characteristics of the database

ABCflux includes 244 sites and 6309 monthly observations, out of which 136 sites and 2217 monthly observations are located in the tundra (54 % of sites and 52 % of observations from North America, 46 % and 48 % from Eurasia), while 108 sites and 4092 monthly observations are located in the boreal biome (59 % of sites and 58 % of observations from North America, 41 % and 42 % from Eurasia) (Table 3). The largest source of flux data are the flux repositories (48 % of the monthly observations), while flux data extracted from papers or contributed by site PIs amount to 30 % and 22 % of the monthly observations, respectively. The database primarily includes sites in unmanaged ecosystems, but it does contain a small number (6) of sites in managed forests.

**Table 3. General statistics of the database. Number of monthly CO<sub>2</sub> flux measurements and sites derived from eddy covariance, chamber, and diffusion techniques, and the proportion of data coming from different data sources. Note that some of the data extracted from flux repositories and papers were further edited by the PIs; this information can be found in the database. For this table, observations that were fully contributed by the PI were considered as PI-contributed.**

Flux measurement technique	Number of sites	Number of <b>monthly</b> observations	Number of <b>monthly</b> observations derived using different eddy covariance and chamber techniques	Number of <b>monthly</b> observations extracted from different data sources
Eddy covariance	Total: 119 Tundra: 47 Boreal: 72	Total: 4957 Tundra: 1406 Boreal: 3551	Open-path: 1988 Closed path: 2085 Both: 245 Enclosed: 240 No information available: 399	Flux repository: 2775 Published: 810 PI-contributed: 1350
Chamber	Total: 104 Tundra: 73 Boreal: 31	Total: 1166 Tundra: 708 Boreal: 458	Manual: 435 Automated: 696 No information available: 35	Flux repository: 243 Published: 901 PI-contributed: 22
Diffusion	Total: 21 Tundra: 16 Boreal: 5	Total: 186 Tundra: 103 Boreal: 83		Flux repository: 0 Published: 186 PI-contributed: 0

Formatted Table

The majority of observations in ABCflux have been measured with the eddy covariance technique (119 sites and 4957 monthly observations), whereas chambers and diffusion methods were used at 125 sites and 1352 observations (Table 3). About 46 % of the eddy covariance measurements are based on gas analyzers using closed-path technology (including enclosed

analyzers), 40 % are based on open-path technology, 5 % include both and 8 % are unknown. 52 % of chamber measurements were automated chambers (monitoring the fluxes continuously throughout the growing season). Only 3 % of the measurements were completed using diffusion methods during the winter. Chamber and diffusion studies were primarily from the tundra and the sparsely treed boreal wetlands, but a few studies with ground surface CO<sub>2</sub> fluxes from forests (i.e., capturing the ground cover vegetation and not the whole ecosystem) are also included in their own fields so that they can not be mixed up with ecosystem-scale measurements (“[Ground\\_NEE\\_gC\\_m2ground\\_nec](#)”, “[Ground\\_GPP\\_gC\\_m2ground\\_gpp](#)”, “[Ground\\_Reco\\_gC\\_m2ground\\_reco](#)”). Further, a few soil CO<sub>2</sub> flux sites measuring fluxes primarily on unvegetated surfaces during the non-growing season are included in the database (“[Rsoil\\_gC\\_m2rsoil](#)”). These were included in the database because ground surface or soil fluxes during the non-growing season can be of similar magnitude to the ecosystem-level fluxes when trees remain dormant (Ryan et al., 1997; Hermle et al., 2010). Therefore, these ground or soil fluxes could potentially be used to represent ecosystem-level fluxes during some of the non-growing season months. However, we did not make an extensive literature search for these observations, rather we compiled observations if they came up in our NEE search. Therefore, the data in these ground surface and soil flux columns represents only a portion of such available data across the ABZ.

The geographical coverage of the flux data is highly variable across the ABZ, with most of the sites and monthly observations coming from Alaska (37 % of the sites and 28 % of the monthly observations), Canada (19 % and 29 %), Finland (7 % and 15 %), and Russia (14 % and 13 %) (Fig. 3). The sites cover a broad range of vegetation types, but were most frequently measured in evergreen needleleaf forests (23 % of the sites and 37 % of the monthly observations) and wetlands in the tundra or boreal zone (30 % and 27 %) (Fig. 4). The northernmost and southernmost ecosystems had fewer sites and observations than more central ecosystems (barren tundra: 45 % of the sites and 3 % of the monthly observations, prostrate shrub: 2 % and <1 %, deciduous broadleaf forest: 1 % and 3 %, deciduous needleleaf forest: 5 % and 4 %, mixed forest <1 % and <1 %). [The sites in ABCflux cover the most frequent climatic conditions across the Arctic-Boreal zone relatively well; however, conditions with high precipitation and low](#)

[temperatures are lacking sites \(Fig. 5\)](#). ABCflux includes sites experiencing various types of disturbances, with the majority of disturbed sites encountering fires (24 sites and 901 monthly observations), thermokarst (4 sites and 113 monthly observations), or harvesting (6 sites and 258 monthly observations). However, ABCflux is dominated by sites in relatively undisturbed environments or sites lacking disturbance information (only 20 % of the sites and 30 % of the monthly observations include disturbance information).

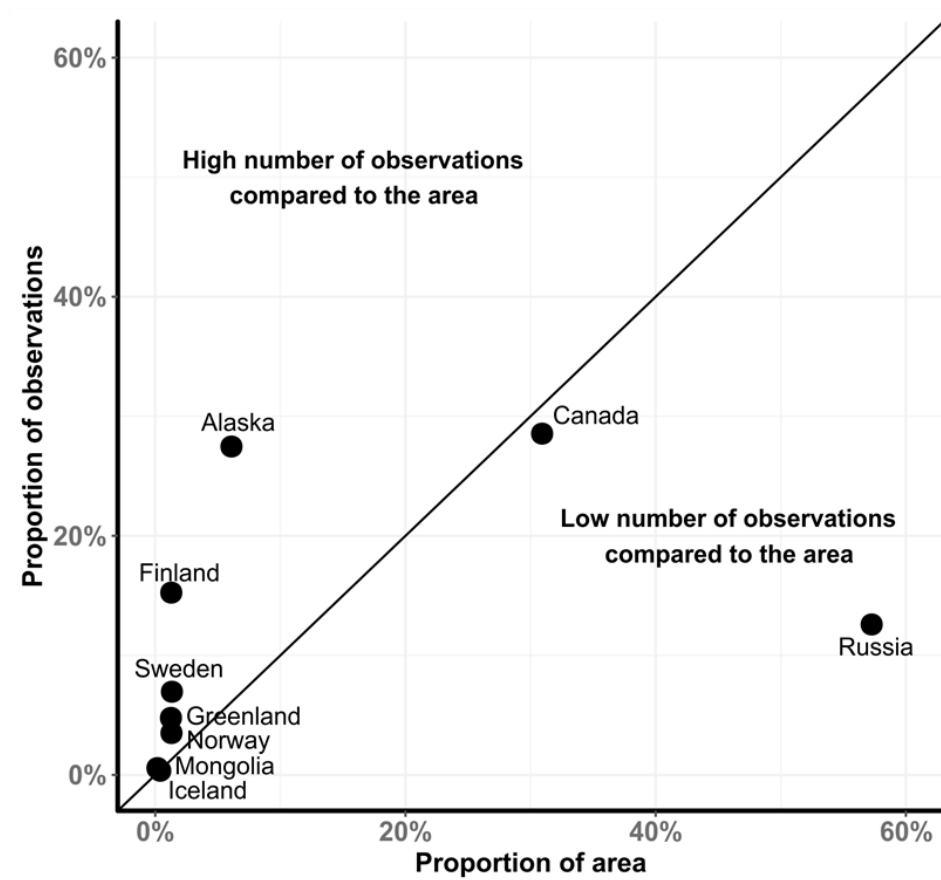
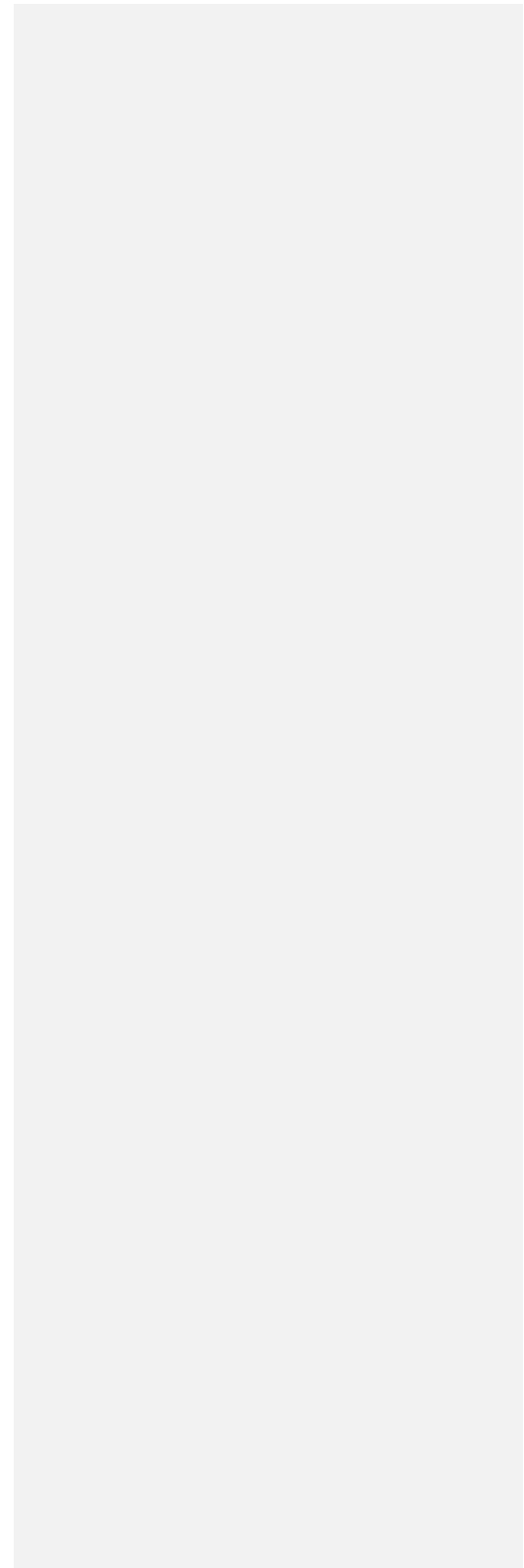
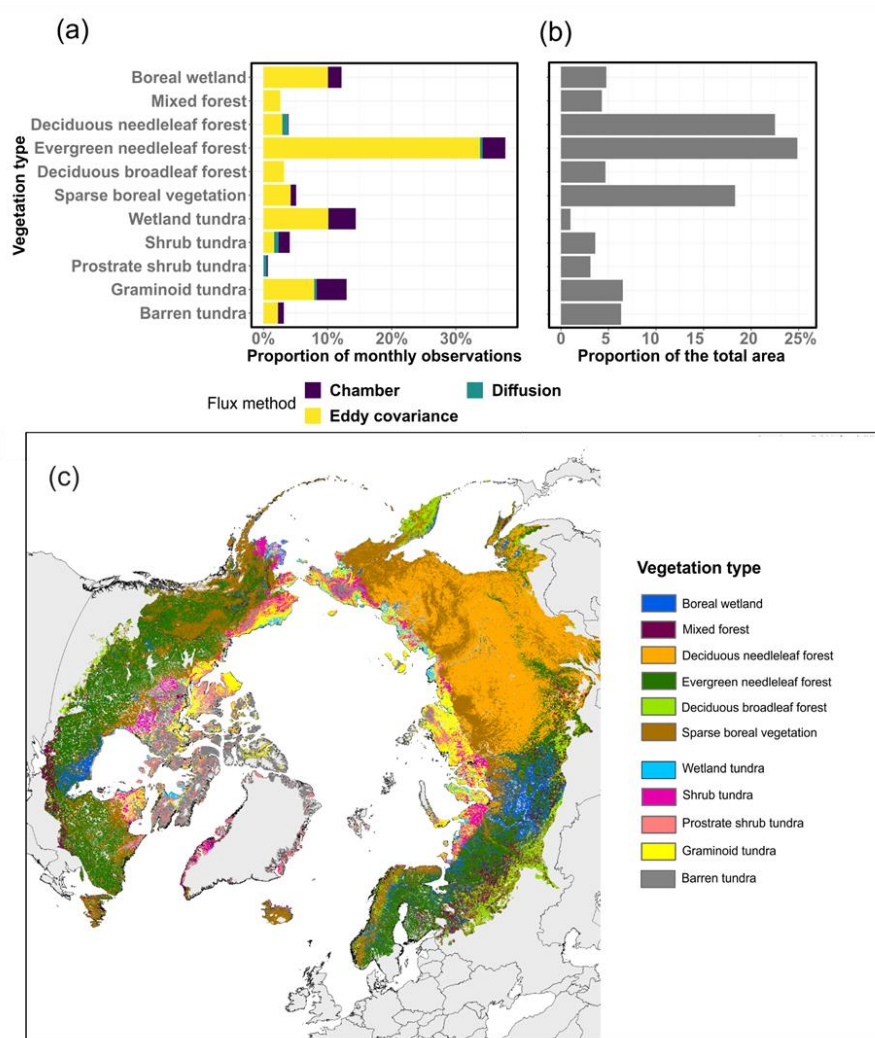


Fig 3. The proportion of monthly observations in each country/region compared to the proportion of the areal extent of the country/region across the entire Arctic-Boreal Zone. Ideally, points would

be close to the 1:1 line (i.e., large countries/regions have more observations than small countries/regions). Permanent water bodies, glaciers, croplands, and urban areas were masked from the areal extent calculation.





**Fig 4.** The proportion of monthly observations in each vegetation type colored by the flux measurement technique (a) and the proportion of the areal extent of each vegetation type across the entire Arctic-Boreal Zone (b). Permanent water bodies, croplands, and urban areas were masked from the areal extent calculation. Sparse boreal vegetation class in the vegetation map includes vegetation mixtures and mosaics.

ABCflux spans a total of 31 years (1989-2020), but the largest number of monthly observations originate from 2000-2015 (80 % of the data) (Fig. 5<sup>6</sup>). The reason for a decrease in flux data over 2015-2020 is likely related to a reporting lag, not a decrease in flux sites and records. The largest number of measurements were conducted during the summer (June-August; 32 %) and the least during the winter (November-February; 18 %) (Fig. 5 and 6). The overall eddy covariance data quality and gap-filled data percentage were lowest during the winter compared to other seasons (0.76 compared to 0.8-0.85 for overall data quality, 0=extensive gap-filling, 1=low gap-filling; 69 % compared to 47 to 59 % for gap-filled data percentage).

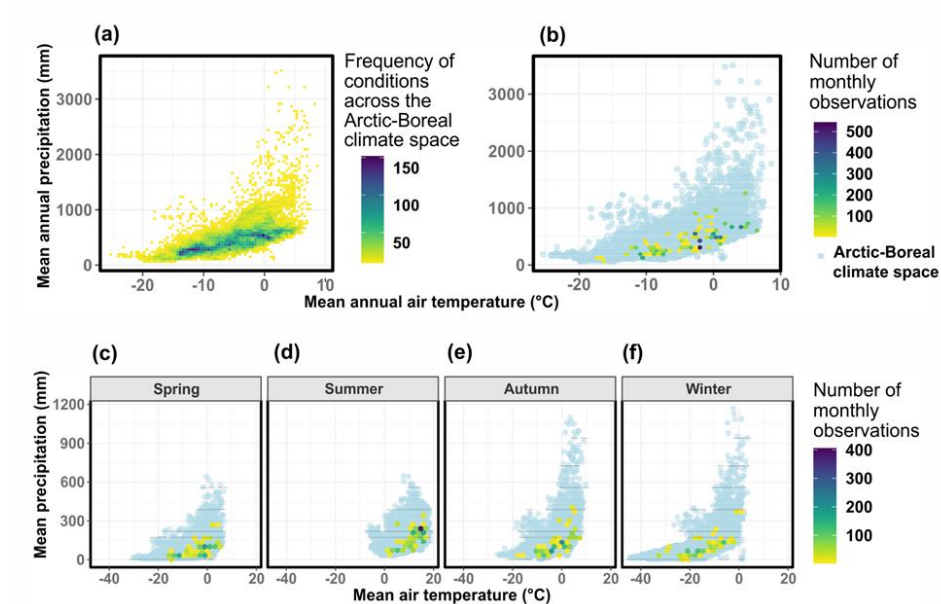


**Fig 5. Mean annual air temperature and precipitation conditions across the Arctic-Boreal zone (a), the entire ABCflux (b), and the air temperature and precipitation conditions across the different climatological seasons included in ABCflux (c-f). Arctic-Boreal climate space was defined based on a random sample of 20000 pixels across the domain.**

Formatted: Not Highlight

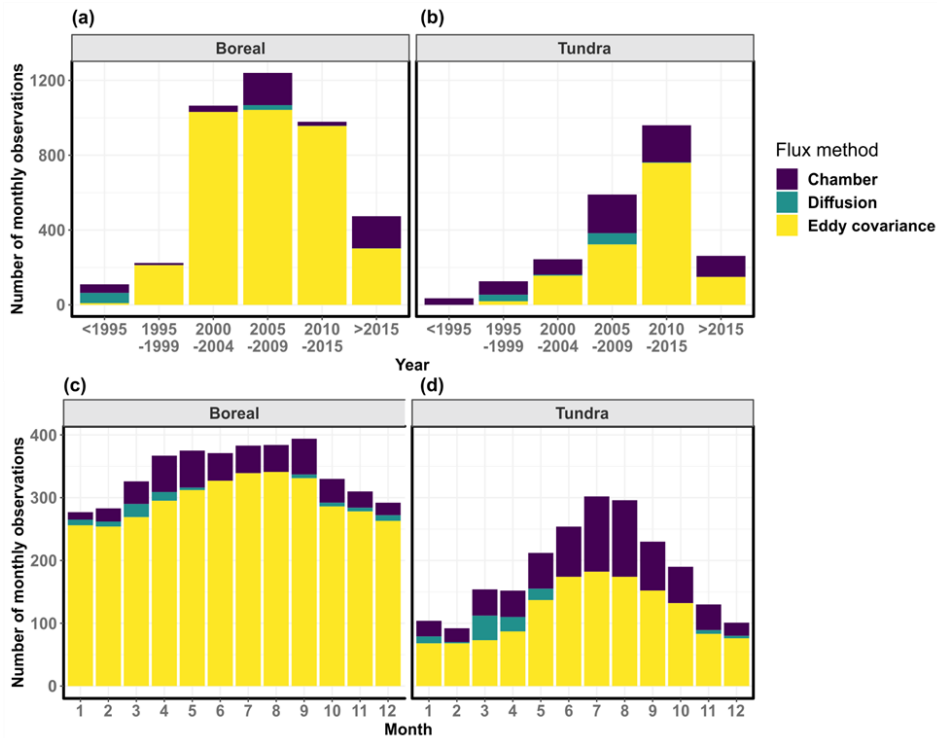


**Fig 6.** Histograms showing the number of monthly measurements across five-year periods (a-b) and across months (c-d) across the tundra and boreal biomes (b). The bar plots are colored by the flux measurement technique. Chambers in the boreal biome measured fluxes in treeless or sparsely treed areas (primarily wetlands).

### 3.2. Coverage of ancillary data

All of the observations in ABCflux include information describing the site name, location, vegetation type, NEE, measurement technique (eddy covariance/chamber/diffusion), and how the



data were compiled (Table 2). Details about the measurement technique (e.g., open or closed-path eddy covariance, manual or automated chambers) are included in 93 % of sites and 93 % of monthly observations. Most of the monthly observations further include information about permafrost extent ( 67 % of the sites and 72 % of the monthly observations), or soil moisture state (47 % of the sites and 56 % of the monthly observations). Data describing air temperature, soil temperature, precipitation, and soil moisture are included in 71, 73, 37, and 35 % of monthly observations, respectively. Some ancillary variables have low data coverage, such as soil organic carbon stocks (16 % of the monthly observations) or active layer thickness (15 % of the monthly observations).

### 3.3. Coverage and distribution of flux data

There are 110 sites and 4290 monthly observations for GPP, 121 sites and 4603 monthly observations for Reco, and 212 sites and 5759 monthly observations for NEE in ABCflux. Monthly values range from -2 to -516 g C m<sup>-2</sup> month<sup>-1</sup> for GPP, from 0 to 550 g C m<sup>-2</sup> month<sup>-1</sup> for Reco, and from -376 to 95 g C m<sup>-2</sup> month<sup>-1</sup> for NEE (Table 4). NEE is typically negative during the summer (i.e., net CO<sub>2</sub> sink) and mostly positive during other seasons (i.e., net CO<sub>2</sub> source) (Fig.-67). Out of all site and year combinations, annual cumulative NEE (the sum of monthly NEE values for each year and site) can be calculated for 267 site-years. An average annual NEE calculated based on the site-level averages from 1995 to 2020 is -27.9 g C m<sup>-2</sup> year<sup>-1</sup> (SD 85.4) for the entire region, -35.5 g C m<sup>-2</sup> year<sup>-1</sup> (SD 93.7) for the boreal biome, and -3.3 g C m<sup>-2</sup> year<sup>-1</sup> (SD 44.2) for the tundra. However, these averages do not account for the spatial or temporal distribution of the observations, and therefore represent coarse summaries of the database.

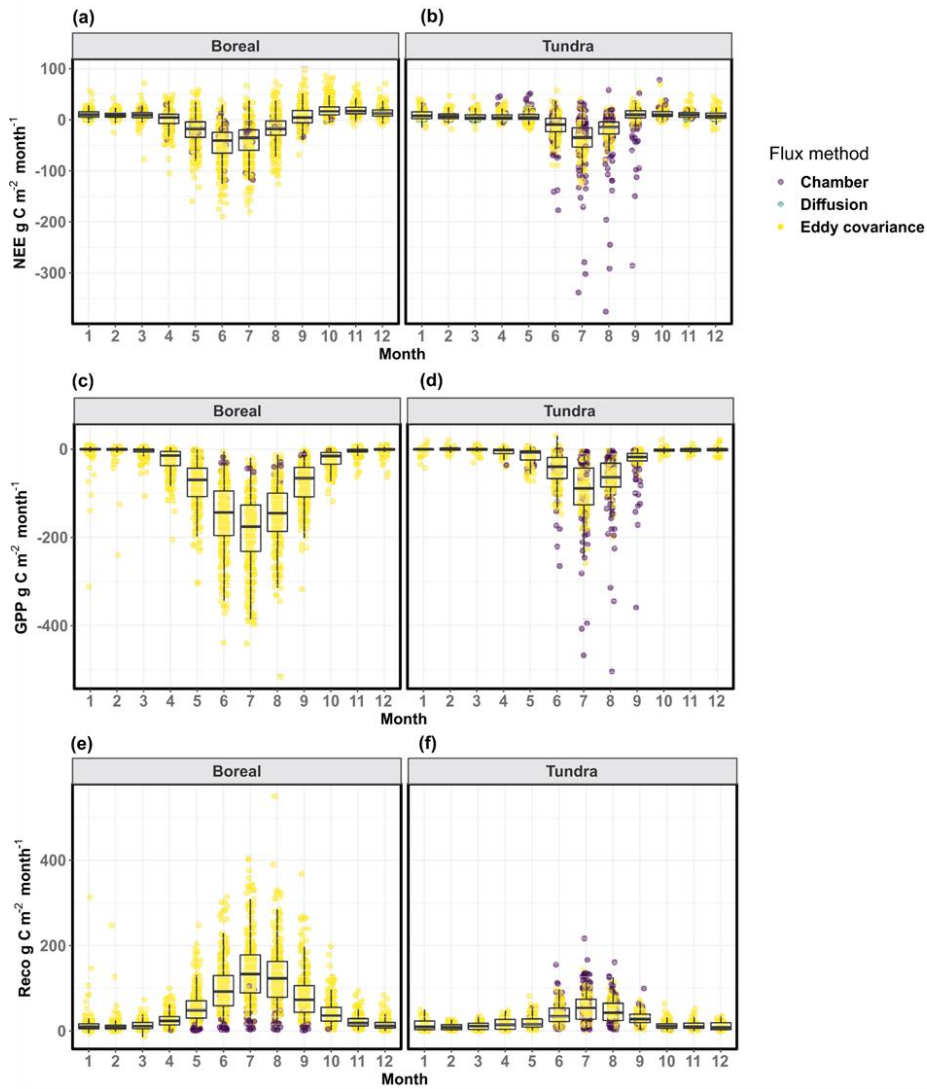


**Fig 67.** The distribution of net ecosystem exchange (NEE; **a-b**), gross primary productivity (GPP; **c-d**), and ecosystem respiration (Reco; **e-f**) across the months **and biomes**, colored by the flux measurement technique. Positive numbers for NEE indicate net CO<sub>2</sub> loss to the atmosphere (i.e., CO<sub>2</sub> source) and negative numbers indicate net CO<sub>2</sub> uptake by the ecosystem (i.e., CO<sub>2</sub> sink). For

consistency, GPP is presented as negative values and Reco as positive. The boxes correspond to the 25th and 75th percentiles. The lines denote the 1.5 IQR of the lower and higher quartile, where IQR is the inter-quartile range, or distance between the first and third quartiles. There is not much chamber data from the boreal regions as they capture NEE only at treeless wetlands.

**Table 4. Mean and standard deviation of monthly observations of net ecosystem exchange (NEE), gross primary productivity (GPP), and ecosystem respiration (Reco) in g C m<sup>-2</sup> month<sup>-1</sup>. Seasons were defined based on the climatological definition (autumn: September-November; winter: December-February; spring: March-May; summer: June-August). Positive numbers for NEE indicate net CO<sub>2</sub> loss to the atmosphere (i.e., CO<sub>2</sub> source) and negative numbers indicate net CO<sub>2</sub> uptake by the ecosystem (i.e., CO<sub>2</sub> sink). For consistency, GPP is presented as negative values and Reco as positive.**

- Some sites compute only NEE and, consequently, NEE summaries might not entirely match with GPP and Reco statistics.

Biome	Climatological season	Mean monthly NEE	Mean monthly GPP	Mean monthly Reco	Standard deviation of monthly NEE	Standard deviation of monthly GPP	Standard deviation of monthly Reco
Boreal	spring	-5	-40	34	25	49	32
Boreal	summer	-35	-163	124	36	79	71
Boreal	autumn	14	-38	52	18	45	46

Boreal	winter	11	-3	14	8	19	20
Tundra	spring	6	-11	18	9	16	14
Tundra	summer	-26	-72	48	38	60	30
Tundra	autumn	10	-14	21	21	30	15
Tundra	winter	9	-2	12	10	9	11

Formatted: Font: (Default) Arial, 11 pt, Not Highlight

Formatted: Font: (Default) Arial

<u>Biome</u>	<u>Climatological season</u>	<u>Mean monthly NEE (standard deviation)</u>	<u>Mean monthly GPP (standard deviation)</u>	<u>Mean monthly Reco (standard deviation)</u>
Boreal	spring	-5 (25)	-40 (49)	34 (32)
Boreal	summer	-35 (36)	-163 (79)	124 (71)
Boreal	autumn	14 (18)	-38 (45)	52 (46)
Boreal	winter	11 (8)	-3 (19)	14 (20)

Tundra	spring	6 (9)	-11 (16)	18 (14)
Tundra	summer	-26 (38)	-72 (60)	48 (30)
Tundra	autumn	10 (21)	-14 (30)	21 (15)
Tundra	winter	9 (10)	-2 (9)	12 (11)

#### 4. Strengths, limitations, and opportunities

ABCflux provides several opportunities for an improved understanding of the ABZ carbon cycle. It can be used to calculate both short- and longer-term monthly, seasonal, or annual flux summaries for different regions, or it can be combined with remote sensing and other gridded data sets to build monthly statistical and process-based models for CO<sub>2</sub> flux upscaling. ABCflux can further be utilized to study the inter- and intra-annual CO<sub>2</sub> flux variability resulting from climate and environmental change. The site distribution in ABCflux can also be used to evaluate the extent of the current flux network and identify under-sampled regions. From a methodological perspective, data users can compare fluxes estimated with the different measurement techniques which can help understand the uncertainties associated with individual techniques. However, there are also some uncertainties that the data user should be aware of when using ABCflux, which we describe below.

##### 4.1. Comparing fluxes estimated with different techniques

The ABCflux database comprises aggregated observations using eddy covariance, chamber, and diffusion methods. These methods measure CO<sub>2</sub> fluxes at different spatiotemporal resolutions and are based on different assumptions. The eddy covariance technique is currently the primary method to monitor long-term trends in ecosystem CO<sub>2</sub> fluxes (Baldocchi et al., 2018; Baldocchi, 2008), and the majority of observations in ABCflux (79 %) have been made using the technique.

Transforming high-frequency eddy covariance measurements to budgets includes several processing steps that can, without harmonization and standardization of these steps (Baldocchi et al., 2001; Pastorello et al., 2020), lead to highly different budget estimates (Soloway et al., 2017). It is also important to acknowledge that the extent and size of the tower footprint differs across the sites due to differences in the height of the tower and the direction and magnitude of the wind (Chu et al., 2021). When fluxes are aggregated over longer time periods to cumulative budgets, one generally assumes the tower footprint remains relatively constant, capturing fluxes from a similar part of the ecosystem (i.e., the assumption that monthly observations within one site in ABCflux can be reliably compared with each other); but note that at shorter time periods this might not be the case (Pirk et al., 2017; Chu et al., 2021).

The different gas analyzer technologies also play an important role for the fluxes estimated with the eddy covariance technique. Sites located in the most northern and remote parts of the ABZ experience a drop in irradiation during autumn and winter which limits solar power availability for eddy covariance measurements. Closed-path systems require more power to run than open-path sensors, but open-path sensors are known to have larger uncertainties. For example, open-path eddy covariance sensors have been shown to incorrectly estimate NEE due to the self-heating effect of the analyzer, which can result in systematically higher net CO<sub>2</sub> uptake compared to closed-path sensors (Kittler et al., 2017a); however, this pattern was not clearly observed in ABCflux when across-site comparisons were made. Furthermore, wintertime fluxes indicating CO<sub>2</sub> uptake can be erroneous due to the limited ability of the gas analyzer to resolve very high frequency turbulent eddies (Jentsch et al., 2021). Recently, some types of open-path infrared gas analysers have been found to be prone to biases in NEE that scale with sensible heat fluxes in all seasons rather than with self-heating (Wang et al., 2017; Helbig et al., 2016).

While using eddy covariance to estimate small-scale spatial variability in NEE is challenging (McGuire et al., 2012), this can be accomplished with chamber and diffusion techniques. Chamber measurements can be done in highly heterogeneous environments as long as chamber closure can be guaranteed; however, most of the chamber measurements in ABCflux have been

conducted in relatively flat and homogeneous graminoid- and wetland-dominated vegetation types. Most chamber sites in ABCflux include ca.10-20 individual plots in total from ca. 3-5 land cover types where fluxes are being measured (Virkkala et al., 2018). Chambers can also provide more direct estimates of Reco and GPP relative to eddy covariance-derived fluxes, and are therefore useful for estimating the magnitude and range of those component fluxes. However, manual chamber and diffusion measurements are laborious and have limited temporal representation, particularly during the non-growing season when they often have only one monthly temporal replicate in ABCflux (McGuire et al., 2012; Fox et al., 2008). Automated chamber measurements during the non-growing season are also rare in ABCflux. Furthermore, uncertainty around gap-filled monthly chamber fluxes is presumably larger than that of the eddy covariance because of the low temporal replication of chamber measurements. Manual chamber measurements might, for example, be conducted during a limited period which does not cover the range of meteorological and phenological conditions within a month. Additional uncertainties in chamber measurements include, for example, accurate determination of chamber volume, pressure perturbations, temperature increase during the measurement, and collars disturbing the ground and causing plant root excision.

Because of these methodological differences across the eddy covariance, chamber and diffusion techniques, comparing fluxes between the methods may result in inconsistencies (Fig. 67). It has been shown that chamber measurements can be both larger or smaller than the fluxes estimated with eddy covariance (Phillips et al., 2017). This difference can be related to the uncertainties with the eddy covariance or chamber technique as described above, ~~or to the uncertainties with the chamber technique (e.g., accurate determination of chamber volume, pressure perturbations, temperature increase during the measurement, collars disturbing the ground and causing plant root excision).~~ The differences can also be due to the mismatch between the chamber and tower footprints (<1 m vs. 250–3000 m radii over the measurement equipment, respectively) and the difficulty of extrapolating local chamber measurements to landscape scales (Marushchak et al., 2013; Fox et al., 2008). However, several studies have also shown good agreement across the eddy covariance and chamber measurements (Laine et al., 2006; Wang et al., 2013; Eckhardt et al., 2019; Riutta et al., 2007). Potential mismatches may also be due to a bias towards daytime

measurements in manual chamber measurements (see field “~~Diurnal\_coverage~~diurnal\_coverage”). During daytime, plants are actively photosynthesizing whereas respiration is the dominant flux at night (López-Blanco et al., 2017). Presumably because of these day vs. night-time differences, we observed stronger sink strength in manual chamber measurements compared to other flux measurements in ABCflux, even though eddy covariance measurements have also been observed to underestimate night-time CO<sub>2</sub> loss. This underestimation in night-time eddy covariance measurements is due to suppressed turbulent exchange linked to stable atmospheric stratification, and systematic biases due to horizontal advection (Aubinet et al., 2012). Despite these uncertainties, including fluxes estimated with all of these techniques into one database improves the understanding of underlying variability of landscape-scale flux estimates. Indeed, there are roughly 10 sites in ABCflux that include both eddy covariance and chamber/diffusion measurements conducted at the same time. These observations might not have identical site coordinates but they are often very close to each other (<500 m away from each other). Including multiple methods from the same site provides an opportunity to compare estimates from different methods over a larger number of sites.

#### 4.2. Uncertainties in eddy covariance flux partitioning

Monthly Reco and GPP fluxes derived from eddy covariance were primarily estimated using ~~flux partitioning based on night-time Reco based on the assumption that during night, NEE measured at low PAR is equivalent to Reco~~night-time partitioning (Reichstein et al., 2005). Focusing on night-time partitioning ensured that data from older sites using this partitioning method could be included, and that most of the fluxes were standardized using one common partitioning method. However, particularly at sites at higher latitudes of the ABZ, low-light night-time conditions are restricted to rather short periods during summer, limiting the database for assessing Reco rates and therefore increasing uncertainties associated with the night-time partitioning (López-Blanco et al., 2020). Recent research suggests that other methods such as daytime partitioning (Lasslop et al. 2010), and even more recently artificial neural networks (ANN) (Tramontana et al., 2020), might be more accurate methods for flux partitioning by addressing the assumptions from night-time partitioning methods (Pastorello et al., 2020; Papale et al., 2006; Reichstein et al., 2005;



Keenan et al., 2019). Specifically, the assumption of a constant diel temperature sensitivity during night- and daytime might introduce error in eddy covariance-based Reco estimates extrapolated from night-time measurements (Järveoja et al., 2020; Keenan et al., 2019). It should be noted that ABCflux database used night-time partitioning of fluxes extracted from repositories for consistency; however, fluxes contributed by some databases, PIs or extracted from papers may be based on other partitioning methods, as noted in the database. In a few cases, observations from the same site were based on different partitioning methods, which limits the usage of data at those sites for time-series exploration. These different gap-filling and partitioning approaches can impact the magnitude of monthly CO<sub>2</sub> budgets. For example, a study comparing four gap-filling methods in a boreal forest showed that the 14-year average annual NEE budget varied from 4 to 48 g C m<sup>-2</sup> year<sup>-1</sup> depending on the gap-filling approach (Soloway et al., 2017). However, a comparison of multiple gap-filling and partitioning methods across sites showed that variation in annual GPP and Reco between partitioning methods was small (Desai et al., 2008), which provides confidence in estimates from partitioned GPP and Reco components from the differing methods used in this database.

We

Any one choice in gap-filling and partitioning introduces uncertainties, and to understand and minimize those uncertainties remains an important research priority. However, since this database was not designed for detailed explorations of how the different gap-filling and partitioning approaches influence fluxes, we recommend users interested in those to access these data in flux repositories or contact site PIs. Fluxes calculated using multiple gap-filling techniques may be considered in the next versions of ABCflux. We further suggest data users remain cautious when using ABCflux data to understand mechanistic relationships between meteorological variables and fluxes, as the gap-filled and partitioned monthly fluxes already include some information about, for example, air or soil temperatures and light conditions. To

completely avoid circularity in these exploratory analyses, we recommend data users download the original and non-gap filled NEE records, or download fluxes partitioned in a way that is consistent and biologically relevant for the particular research question from flux repositories.

#### 4.3. Representativeness and completeness of the data

The ABCflux database site distribution covers all vegetation types and countries within the ABZ. However, there are regional and temporal biases in the database due to the differences in accessibility for sampling certain regions (also documented in ~~(Virkkala et al., 2019, 2019; Pallandt et al. 2021)~~). As a result, the number of monthly observations does not always correlate with the size of the country/region or vegetation type. For example, Russia and Canada cover in total ca. 80 % of the ABZ but include only ca. 40 % of the monthly observations. While the distribution of these measurements ~~seems to be~~ rather balanced between the Russian tundra and boreal biomes, Canadian observations are primarily located in the boreal biome, largely due to the high amount of measurements conducted as part of the [NASA Boreal Ecosystem-Atmosphere Study](#) (Sellers et al., 1997). Deciduous needleleaf (i.e., larch) forests, the primary vegetation type in central and eastern Siberia, has the smallest amount of data compared to its area (<5 % of monthly observations vs. >20 % coverage of the ABZ). Additional data gaps are located in barren and prostrate-shrub tundra and sparse boreal vegetation, as well as in areas with high precipitation. Eddy covariance towers in mountainous regions are also rare- (Pallandt et al. 2021) as eddy covariance towers are most often set up over homogeneous and flat terrains to avoid advection (Baldocchi, 2003; Etzold et al., 2010). Alaska and Finland cover <10 % of the ABZ but include >40 % of the monthly observations.

There are differences in environmental coverage of ABCflux depending on the measured flux, measurement year, and the measurement season. Sites with NEE observations have the largest geographical coverage, with less availability for partitioned GPP and Reco fluxes. Therefore, regional summaries of Reco and GPP do not sum up to NEE. Moreover, although the oldest records in ABCflux originate from 1989, observations from the 1990s are primarily located in a

Formatted: Underline

Formatted: Underline

Formatted: Underline

few boreal or Alaskan tundra sites. The measurement records from tundra sites are shorter than boreal sites over the full time span of the database, and it is therefore more uncertain to investigate long-term temporal changes in tundra fluxes. Finally, the lowest amount of flux data in ABCflux is ~~from~~during winter, which is the most challenging period for data collection in high latitudes (Kittler et al., 2017b; Jentsch et al., 2021). [Autumn and winter data included in ABCflux further covers a smaller Arctic-Boreal climate space, with no data coming from extremely cold or wet conditions \(Fig. 5\)](#). Fluxes are generally small during this period (Natali et al., ~~2019~~2019a), leading to higher relative uncertainties in flux estimation compared to other seasons. These regional and temporal biases need to be considered in future analyses to assure the robustness of our understanding of  $C_{carbon}$  fluxes across the ABZ.

Although ABCflux includes a comprehensive compilation of flux and supporting environmental and methodological information, the information is not exhaustive. We acknowledge that this database is missing some eddy covariance sites that were recently summarized in a tower survey (see preliminary results in <https://cosima.nceas.ucsb.edu/carbon-flux-sites/>), because these data were unavailable at the time of database compilation. Moreover, the overall quality or the gap-filled percentage of the eddy covariance observations is not reported for each eddy covariance site, limiting the potential to explore the effects of data quality on fluxes across all the eddy covariance sites. Comparing soil temperature or moisture across sites has uncertainties due to differences in sensor depths, which are not always reported in the database. We hope to improve and increase the flux and supporting data in the future as new data are being collected, for example, by leveraging the ONEflux pipeline and its different outputs (Pastorello et al., 2020), as well as aggregating new measurements that are not part of any networks.

## 5. Data use guidelines

Data are publicly available using a Creative Commons Attribution 4.0 International copyright (CC BY 4.0). Data are fully public, but should be appropriately referenced by citing this paper and the database (see Section 6). We suggest that researchers planning to use this database as a core dataset for their analysis contact and collaborate with the database developers and relevant individual site contributors.

## **6. Data availability and access**

The database associated with this publication can be found at Virkkala et al. 2021a (<https://doi.org/10.3334/ORN LDAAC/1934>).

## **7. Conclusions**

ABCflux provides the most comprehensive database of ABZ terrestrial ecosystem CO<sub>2</sub> fluxes to date. It is particularly useful for future modeling, remote sensing, and empirical studies aiming to understand CO<sub>2</sub> budgets and regional variability in flux magnitudes, as well as changes in fluxes through time. It can also be used to understand how different environmental conditions influence fluxes, and to better understand the current extent of the flux measurement network and its representativeness across the Arctic-Boreal region.

## **8. Author contributions**

The ABCflux database was conceptualized and developed by a team led by SMN, BMR, JDW, MM, AMV, and EAGS, with additional comments from OS. KS and SJC compiled the data, with contributions from AMV, MM, DP, CM, and JN, and data screening by AMV and SMN. AMV drafted and coordinated the manuscript in close collaboration with SMN, BMR, JDW, KS, and MM. All authors contributed to the realization of the ABCflux database and participated in the editing of the manuscript. PIs whose data were extracted from publications are not coauthors in this paper, unless new data were provided, but their contact details can be found in the database.

## **9. Competing interests**

The authors declare that they have no conflict of interest.

## **10. Acknowledgements**

AMV, BMR, SMN, and JDW were funded by the Gordon and Betty Moore Foundation (grant #8414). BMR, KS, SJC, CM, and JN were also funded by the NASA Carbon Cycle Science and Arctic-Boreal Vulnerability Experiment programs (ABoVE grant NNX17AE13G), SMN by NASA ABoVE (grant NNX15AT81A) and JDW by NNX15AT81A and NASA NIP grant

NNH17ZDA001N. EAGS acknowledges NSF Research, Synthesis, and Knowledge Transfer in a Changing Arctic: Science Support for the Study of Environmental Arctic Change (grant #1331083) and NSF PLR Arctic System Science Research Networking Activities (Permafrost Carbon Network: Synthesizing Flux Observations for Benchmarking Model Projections of Permafrost Carbon Exchange; grant #1931333. EAGS further acknowledges US Department of Energy and Denali National Park. MBN and MP acknowledge Swedish ICOS (Integrated Carbon Observatory System) funded by VR and contributing institutions; SITES (Swedish Infrastructure for Ecosystem Science) funded by VR and contributing institutions; VR (grant # 2018-03966 and # 2019-04676), FORMAS (grant # 2016-01289), and Kempe Foundations (SMK-1211). EE, CE, and MSB-H was funded by NSF Arctic Observatory Network and CAG, VSL, EH by Natural Sciences and Engineering Research Council. IM, PK, EST, AL acknowledges ICOS-Finland and AV Russian Science Foundation, project 21-14-00209. AL, MA, TL, J-PT, and JH further acknowledge Ministry of transport and communication. WQ, EE, VSL were funded by ArcticNet. HK acknowledges The Arctic Challenge for Sustainability and The Arctic Challenge for Sustainability II (JPMXD1420318865), MEM the Academy of Finland project PANDA (decision no. 317054) and CV the Academy of Finland project MUFFIN (decision no. 332196). NN acknowledges Arctic Data Center, National Science Foundation, US Department of Energy, Denali National Park. YM was funded by Ministry of Environment, Japan and MU by the Arctic Challenge for Sustainability II (ArCS II; JPMXD1420318865) and KAKENHI (19H05668). SFO acknowledges US National Science Foundation, and MiM, BE, TRC Greenland Ecosystem Monitoring program. BE further acknowledge Arctic Station, University of Copenhagen and the Danish National Research Foundation (CENPERM DNR100). ELB was funded by "Greenland Research Council, grant number 80.35, financed by the "Danish Program for Arctic Research", and LM by TCOS Siberia. DH and LK were funded by Deutsche Forschungsgemeinschaft under Germany's Excellence Strategy – EXC 177 'CliSAP - Integrated Climate System Analysis and Prediction'. JJ acknowledges Swedish Forest Society Foundation (2018-485-Steig 2 2017) and FORMAS (2018-00792). DZ was funded by National Science Foundation (NSF) (award number 1204263, and 1702797) NASA ABoVE (NNX15AT74A; NNX16AF94A) Program, Natural Environment Research Council (NERC) UAMS Grant (NE/P002552/1), NOAA Cooperative Science Center for Earth System Sciences and Remote Sensing Technologies (NOAA-CESSRST) under the Cooperative Agreement Grant # NA16SEC4810008, European Union's

Horizon 2020 research and innovation program under grant agreement No. 72789. S-JP was funded by National Research Foundation of Korea Grant from the Korean Government (NRF-2021M1A5A1065425, KOPRI-PN21011). NC acknowledges "National Research Foundation of Korea Grant from the Korean Government (MSIT; the Ministry of Science and ICT) (NRF-2021M1A5A1065679 and NRF-2021R111A1A01053870)". SD was funded by Department of Energy and NGEA- Arctic. FJWP is funded by the Swedish Research Council (registration nr. 2017-05268) and the Research Council of Norway (grant no. 274711). ~~The authors would like to acknowledge Tiffany Windholz for her work on standardizing and cleaning up the database.~~

~~**References** ASP and VIZ were funded by grant of the Russian Fund for Basic Research # 18-05-60203-Arktika. The authors would like to acknowledge Tiffany Windholz for her work on standardizing and cleaning up the database.~~

## References

Abatzoglou, J. T., Dobrowski, S. Z., Parks, S. A., and Hegewisch, K. C.: TerraClimate, a high-resolution global dataset of monthly climate and climatic water balance from 1958-2015, Sci Data, 5, 170191, <https://doi.org/10.1038/sdata.2017.191>, 2018.

Natural Earth - Free vector and raster map data at 1:10m, 1:50m, and 1:110m scales: <https://www.naturalearthdata.com/>, last access: 12 February 2021.

Reconciling historical and contemporary trends in terrestrial carbon exchange of the northern permafrost-zone: <https://arcticdata.io/reconciling-historical-and-contemporary-trends-in-terrestrial-carbon-exchange-of-the-northern-permafrost-zone/>, last access: 11 February 2021.

Aubinet, M., Vesala, T., and Papale, D.: Eddy Covariance: A Practical Guide to Measurement and Data Analysis, Springer Science & Business Media, 438 pp., 2012.

Aurela, M., Laurila, T., and Tuovinen, J. P.: Annual CO<sub>2</sub> balance of a subarctic fen in northern Europe: Importance of the wintertime efflux, J. Geophys. Res., 2002.

Bäckstrand, K., Crill, P. M., Jackowicz-Korczyński, M., Mastepanov, M., Christensen, T. R., and Bastviken, D.: Annual carbon gas budget for a subarctic peatland, Northern Sweden, <https://doi.org/10.5194/bg-7-95-2010>, 2010.

Baldocchi, D.: "Breathing" of the terrestrial biosphere: lessons learned from a global network of carbon dioxide flux measurement systems, Aust. J. Bot., 56, 1–26, 2008.

Formatted: Font: 12 pt, Not Bold

Baldocchi, D., Falge, E., Gu, L., Olson, R., Hollinger, D., Running, S., Anthoni, P., Bernhofer, C., Davis, K., Evans, R., Fuentes, J., Goldstein, A., Katul, G., Law, B., Lee, X., Malhi, Y., Meyers, T., Munger, W., Oechel, W., Paw U, K. T., Pilegaard, K., Schmid, H. P., Valentini, R., Verma, S., Vesala, T., Wilson, K., and Wofsy, S.: FLUXNET: A New Tool to Study the Temporal and Spatial Variability of Ecosystem-Scale Carbon Dioxide, Water Vapor, and Energy Flux Densities, *Bull. Am. Meteorol. Soc.*, 82, 2415–2434, [https://doi.org/10.1175/1520-0477\(2001\)082<2415:FANTTS>2.3.CO;2](https://doi.org/10.1175/1520-0477(2001)082<2415:FANTTS>2.3.CO;2), 2001.

Baldocchi, D., Chu, H., and Reichstein, M.: Inter-annual variability of net and gross ecosystem carbon fluxes: A review, *Agric. For. Meteorol.*, 249, 520–533, <https://doi.org/10.1016/j.agrformet.2017.05.015>, 2018.

Baldocchi, D. D.: Assessing the eddy covariance technique for evaluating carbon dioxide exchange rates of ecosystems: past, present and future, <https://doi.org/10.1046/j.1365-2486.2003.00629.x>, 2003.

Belshe, E. F., Schuur, E. A. G., and Bolker, B. M.: Tundra ecosystems observed to be CO<sub>2</sub> sources due to differential amplification of the carbon cycle, *Ecol. Lett.*, 16, 1307–1315, <https://doi.org/10.1111/ele.12164>, 2013.

Björkman, M. P., Morgner, E., Björk, R. G., Cooper, E. J., Elberling, B., and Klemetsson, L.: A comparison of annual and seasonal carbon dioxide effluxes between sub-Arctic Sweden and High-Arctic Svalbard, *Polar Res.*, 29, 75–84, <https://doi.org/10.1111/j.1751-8369.2010.00150.x>, 2010a.

Björkman, M. P., Morgner, E., Cooper, E. J., Elberling, B., Klemetsson, L., and Björk, R. G.: Winter carbon dioxide effluxes from Arctic ecosystems: An overview and comparison of methodologies: WINTER CO<sub>2</sub>EFFLUXES FROM ARCTIC SOILS, *Global Biogeochem. Cycles*, 24, <https://doi.org/10.1029/2009gb003667>, 2010b.

Bond-Lamberty, B., Christianson, D. S., Malhotra, A., Pennington, S. C., Sihi, D., AghaKouchak, A., Anjileli, H., Altaf Arain, M., Armesto, J. J., Ashraf, S., Ataka, M., Baldocchi, D., Andrew Black, T., Buchmann, N., Carbone, M. S., Chang, S.-C., Crill, P., Curtis, P. S., Davidson, E. A., Desai, A. R., Drake, J. E., El-Madany, T. S., Gavazzi, M., Görres, C.-M., Gough, C. M., Goulden, M., Gregg, J., Gutiérrez Del Arroyo, O., He, J.-S., Hirano, T., Hoppo, A., Hughes, H., Järveoja, J., Jassal, R., Jian, J., Kan, H., Kaye, J., Kominami, Y., Liang, N., Lipson, D., Macdonald, C. A., Maseyk, K., Mathes, K., Mauritz, M., Mayes, M. A., McNulty, S., Miao, G., Migliavacca, M., Miller, S., Miniati, C. F., Nietz, J. G., Nilsson, M. B., Noormets, A., Norouzi, H., O'Connell, C. S., Osborne, B., Oyonarte, C., Pang, Z., Peichl, M., Pendall, E., Perez-Quezada, J. F., Phillips, C. L., Phillips, R. P., Raich, J. W., Renchon, A. A., Ruehr, N. K., Sánchez-Cañete, E. P., Saunders, M., Savage, K. E., Schrumpf, M., Scott, R. L., Seibt, U., Silver, W. L., Sun, W., Szutu, D., Takagi, K., Takagi, M., Teramoto, M., Tjoelker, M. G., Trumbore, S.,

Ueyama, M., Vargas, R., Varner, R. K., Verfaillie, J., Vogel, C., Wang, J., Winston, G., Wood, T. E., Wu, J., Wutzler, T., Zeng, J., Zha, T., Zhang, Q., and Zou, J.: COSORE: A community database for continuous soil respiration and other soil-atmosphere greenhouse gas flux data, *Glob. Chang. Biol.*, 26, 7268–7283, <https://doi.org/10.1111/gcb.15353>, 2020.

Box, J. E., Colgan, W. T., Christensen, T. R., Schmidt, N. M., Lund, M., Parmentier, F.-J. W., Brown, R., Bhatt, U. S., Euskirchen, E. S., Romanovsky, V. E., Walsh, J. E., Overland, J. E., Wang, M., Corell, R. W., Meier, W. N., Wouters, B., Mernild, S., Mård, J., Pawlak, J., and Olsen, M. S.: Key indicators of Arctic climate change: 1971–2017, *Environ. Res. Lett.*, 14, 045010, <https://doi.org/10.1088/1748-9326/aafc1b>, 2019.

Cahoon, S. M. P., Sullivan, P. F., and Post, E.: Greater Abundance of *Betula nana* and Early Onset of the Growing Season Increase Ecosystem CO<sub>2</sub> Uptake in West Greenland, *Ecosystems*, 19, 1149–1163, <https://doi.org/10.1007/s10021-016-9997-7>, 2016.

Chu, H., Luo, X., Ouyang, Z., Chan, W. S., Dengel, S., Biraud, S. C., Torn, M. S., Metzger, S., Kumar, J., Arain, M. A., Arkebauer, T. J., Baldocchi, D., Bernacchi, C., Billesbach, D., Black, T. A., Blanken, P. D., Bohrer, G., Bracho, R., Brown, S., Brunsell, N. A., Chen, J., Chen, X., Clark, K., Desai, A. R., Duman, T., Durden, D., Fares, S., Forbrich, I., Gamon, J. A., Gough, C. M., Griffis, T., Helbig, M., Hollinger, D., Humphreys, E., Ikawa, H., Iwata, H., Ju, Y., Knowles, J. F., Knox, S. H., Kobayashi, H., Kolb, T., Law, B., Lee, X., Litvak, M., Liu, H., Munger, J. W., Noormets, A., Novick, K., Oberbauer, S. F., Oechel, W., Oikawa, P., Papuga, S. A., Pendall, E., Prajapati, P., Prueger, J., Quinton, W. L., Richardson, A. D., Russell, E. S., Scott, R. L., Starr, G., Staebler, R., Stoy, P. C., Stuart-Haëntjens, E., Sonnentag, O., Sullivan, R. C., Suyker, A., Ueyama, M., Vargas, R., Wood, J. D., and Zona, D.: Representativeness of Eddy-Covariance flux footprints for areas surrounding AmeriFlux sites, *Agric. For. Meteorol.*, 301-302, 108350, <https://doi.org/10.1016/j.agrformet.2021.108350>, 2021.

Desai, A. R., Richardson, A. D., Moffat, A. M., Kattge, J., Hollinger, D. Y., Barr, A., Falge, E., Noormets, A., Papale, D., Reichstein, M., and Stauch, V. J.: Cross-site evaluation of eddy covariance GPP and RE decomposition techniques, *Agric. For. Meteorol.*, 148, 821–838, <https://doi.org/10.1016/j.agrformet.2007.11.012>, 2008.

[Didan, K.: MOD13A3 MODIS/Terra Vegetation Indices Monthly L3 Global 1km SIN Grid V006. https://doi.org/10.5067/MODIS/MOD13A3.006. 2015.](https://doi.org/10.5067/MODIS/MOD13A3.006)

Dinerstein, E., Olson, D., Joshi, A., Vynne, C., Burgess, N. D., Wikramanayake, E., Hahn, N., Palminteri, S., Hedao, P., Noss, R., Hansen, M., Locke, H., Ellis, E. C., Jones, B., Barber, C. V., Hayes, R., Kormos, C., Martin, V., Crist, E., Sechrest, W., Price, L., Baillie, J. E. M., Weeden, D., Suckling, K., Davis, C., Sizer, N., Moore, R., Thau, D., Birch, T., Potapov, P., Turubanova, S., Tyukavina, A., de Souza, N., Pintea, L., Brito, J. C., Llewellyn, O. A., Miller, A. G., Patzelt, A., Ghazanfar, S. A., Timberlake, J., Klöser, H., Shennan-Farþón, Y., Kindt, R., Lillesø, J.-P. B.,



van Breugel, P., Graudal, L., Voge, M., Al-Shammari, K. F., and Saleem, M.: An Ecoregion-Based Approach to Protecting Half the Terrestrial Realm, *Bioscience*, 67, 534–545, <https://doi.org/10.1093/biosci/bix014>, 2017.

Eckhardt, T., Knoblauch, C., Kutzbach, L., Holl, D., Simpson, G., Abakumov, E., and Pfeiffer, E.-M.: Partitioning net ecosystem exchange of CO<sub>2</sub> on the pedon scale in the Lena River Delta, Siberia, *Biogeosciences*, 16, 1543–1562, <https://doi.org/10.5194/bg-16-1543-2019>, 2019.

Etzold, S., Buchmann, N., and Eugster, W.: Contribution of advection to the carbon budget measured by eddy covariance at a steep mountain slope forest in Switzerland, *Biogeosciences*, 7, 2461–2475, <https://doi.org/10.5194/bg-7-2461-2010>, 2010.

Euskirchen, E. S., Bret-Harte, M. S., Scott, G. J., Edgar, C., and Shaver, G. R.: Seasonal patterns of carbon dioxide and water fluxes in three representative tundra ecosystems in northern Alaska, *Ecosphere*, 3, art4, <https://doi.org/10.1890/es11-00202.1>, 2012.

Fox, A. M., Huntley, B., Lloyd, C. R., Williams, M., and Baxter, R.: Net ecosystem exchange over heterogeneous Arctic tundra: Scaling between chamber and eddy covariance measurements, *Global Biogeochem. Cycles*, 22, 2008.

Gorham, E.: Northern Peatlands: Role in the Carbon Cycle and Probable Responses to Climatic Warming, *Ecol. Appl.*, 1, 182–195, <https://doi.org/10.2307/1941811>, 1991.

Hari, P., Nikinmaa, E., Pohja, T., Siivola, E., Bäck, J., Vesala, T., and Kulmala, M.: Station for Measuring Ecosystem-Atmosphere Relations: SMEAR, in: *Physical and Physiological Forest Ecology*, edited by: Hari, P., Heliövaara, K., and Kulmala, L., Springer Netherlands, Dordrecht, 471–487, [https://doi.org/10.1007/978-94-007-5603-8\\_9](https://doi.org/10.1007/978-94-007-5603-8_9), 2013.

[Hayes, D. J., Kicklighter, D. W., David McGuire, A., Chen, M., Zhuang, Q., Yuan, F., Melillo, J. M., and Wullschleger, S. D.: The impacts of recent permafrost thaw on land-atmosphere greenhouse gas exchange. \*Environ. Res. Lett.\*, 9, 045005, <https://doi.org/10.1088/1748-9326/9/4/045005>, 2014.](#)

[Heiskanen, L., Tuovinen, J.-P., Räsänen, A., Virtanen, T., Juutinen, S., Lohila, A., Penttilä, T., Linkosalmi, M., Mikola, J., Laurila, T., and Aurela, M.: Carbon dioxide and methane exchange of a patterned subarctic fen during two contrasting growing seasons, \*Biogeosciences\*, 18, 873–896, <https://doi.org/10.5194/bg-18-873-2021>, 2021.](#)

Helbig, M., Wischniewski, K., Gosselin, G. H., Biraud, S. C., Bogoev, I., Chan, W. S., Euskirchen, E. S., Glenn, A. J., Marsh, P. M., Quinton, W. L., and Sonntag, O.: Addressing a systematic bias in carbon dioxide flux measurements with the EC150 and the IRGASON open-

path gas analyzers, *Agric. For. Meteorol.*, 228-229, 349–359, <https://doi.org/10.1016/j.agrformet.2016.07.018>, 2016.

[Heliasz, M., Johansson, T., Lindroth, A., Mölder, M., Mastepanov, M., Friborg, T., Callaghan, T. V., and Christensen, T. R.: Quantification of C uptake in subarctic birch forest after setback by an extreme insect outbreak, \*Geophys. Res. Lett.\*, 38, <https://doi.org/10.1029/2010gl044733>, 2011.](#)

Hermle, S., Lavigne, M. B., Bernier, P. Y., Bergeron, O., and Paré, D.: Component respiration, ecosystem respiration and net primary production of a mature black spruce forest in northern Quebec, *Tree Physiol.*, 30, 527–540, <https://doi.org/10.1093/treephys/tpq002>, 2010.

Hugelius, G., Strauss, J., Zubrzycki, S., Harden, J. W., Schuur, E. A. G., Ping, C.-L., Schirrmeyer, L., Grosse, G., Michaelson, G. J., Koven, C. D., and Others: Estimated stocks of circumpolar permafrost carbon with quantified uncertainty ranges and identified data gaps, *Biogeosciences*, 11, 2014.

Hugelius, G., Loisel, J., Chadburn, S., Jackson, R. B., Jones, M., MacDonald, G., Marushchak, M., Olefeldt, D., Packalen, M., Siewert, M. B., Treat, C., Turetsky, M., Voigt, C., and Yu, Z.: Large stocks of peatland carbon and nitrogen are vulnerable to permafrost thaw, *Proc. Natl. Acad. Sci. U. S. A.*, 117, 20438–20446, <https://doi.org/10.1073/pnas.1916387117>, 2020.

Järveoja, J., Nilsson, M. B., Gažovič, M., Crill, P. M., and Peichl, M.: Partitioning of the net CO<sub>2</sub> exchange using an automated chamber system reveals plant phenology as key control of production and respiration fluxes in a boreal peatland, *Glob. Chang. Biol.*, 24, 3436–3451, 2018.

Järveoja, J., Nilsson, M. B., Crill, P. M., and Peichl, M.: Bimodal diel pattern in peatland ecosystem respiration rebuts uniform temperature response, *Nat. Commun.*, 11, 4255, <https://doi.org/10.1038/s41467-020-18027-1>, 2020.

Jentzsch, K., Schulz, A., Pirk, N., Foken, T., Crewell, S., and Boike, J.: High levels of CO<sub>2</sub> exchange during synoptic-scale events introduce large uncertainty into the arctic carbon budget, *Geophys. Res. Lett.*, 48, <https://doi.org/10.1029/2020gl092256>, 2021.

Jian, J., Vargas, R., Anderson-Teixeira, K., Stell, E., Herrmann, V., Horn, M., Kholod, N., Manzon, J., Marchesi, R., Paredes, D., and Others: A restructured and updated global soil respiration database (SRDB-V5), 1–19, 2020.

Keenan, T. F. and Williams, C. A.: The Terrestrial Carbon Sink, *Annu. Rev. Environ. Resour.*, 43, 219–243, <https://doi.org/10.1146/annurev-environ-102017-030204>, 2018.

Keenan, T. F., Migliavacca, M., Papale, D., Baldocchi, D., Reichstein, M., Torn, M., and Wutzler, T.: Widespread inhibition of daytime ecosystem respiration, *Nat Ecol Evol*, 3, 407–415, <https://doi.org/10.1038/s41559-019-0809-2>, 2019.

Kittler, F., Eugster, W., Foken, T., Heimann, M., Kolle, O., and Göckede, M.: High-quality eddy-covariance CO<sub>2</sub> budgets under cold climate conditions: Arctic Eddy-Covariance CO<sub>2</sub> Budgets, *J. Geophys. Res. Biogeosci.*, 122, 2064–2084, <https://doi.org/10.1002/2017jg003830>, 2017a.

Kittler, F., Heimann, M., Kolle, O., Zimov, N., Zimov, S., and Göckede, M.: Long-term drainage reduces CO<sub>2</sub> uptake and CH<sub>4</sub> emissions in a Siberian permafrost ecosystem, *Global Biogeochem. Cycles*, 31, 1704–1717, 2017b.

[Lafleur, P. M., Humphreys, E. R., St Louis, V. L., Myklebust, M. C., Papakyriakou, T., Poissant, L., Barker, J. D., Pilote, M., and Swystun, K. A.: Variation in peak growing season net ecosystem production across the Canadian Arctic, \*Environ. Sci. Technol.\*, 46, 7971–7977, <https://doi.org/10.1021/es300500m>, 2012.](https://doi.org/10.1021/es300500m)

Laine, A., Sottocornola, M., Kiely, G., Byrne, K. A., Wilson, D., and Tuittila, E.-S.: Estimating net ecosystem exchange in a patterned ecosystem: Example from blanket bog, *Agric. For. Meteorol.*, 138, 231–243, <https://doi.org/10.1016/j.agrformet.2006.05.005>, 2006.

Lamarche, C., Bontemps, S., Verhegghen, A., Radoux, J., Vanbogaert, E., Kalogirou, V., Seifert, F. M., Arino, O., and Defourny, P.: Characterizing The Surface Dynamics For Land Cover Mapping: Current Achievements Of The ESA CCI Land Cover, 72279, 2013.

Lasslop, G., Reichstein, M., Papale, D., Richardson, A. D., Arneth, A., Barr, A., Stoy, P., and Wohlfahrt, G.: Separation of net ecosystem exchange into assimilation and respiration using a light response curve approach: critical issues and global evaluation: SEPARATION OF NEE INTO GPP AND RECO, *Glob. Chang. Biol.*, 16, 187–208, <https://doi.org/10.1111/j.1365-2486.2009.02041.x>, 2010.

López-Blanco, E., Lund, M., Williams, M., Tamstorf, M. P., Westergaard-Nielsen, A., Exbrayat, J.-F., Hansen, B. U., and Christensen, T. R.: Exchange of CO<sub>2</sub> in Arctic tundra: impacts of meteorological variations and biological disturbance, *Biogeosciences*, 14, 4467–4483, <https://doi.org/10.5194/bg-14-4467-2017>, 2017.

López-Blanco, E., Jackowicz-Korczynski, M., Mastepanov, M., Skov, K., Westergaard-Nielsen, A., Williams, M., and Christensen, T. R.: Multi-year data-model evaluation reveals the importance of nutrient availability over climate in arctic ecosystem C dynamics, *Environ. Res. Lett.*, 15, 094007, <https://doi.org/10.1088/1748-9326/ab865b>, 2020.

Luysaert, S., Inghima, I., Jung, M., Richardson, A. D., Reichstein, M., Papale, D., Piao, S. L., Schulze, E.-D., Wingate, L., Matteucci, G., Aragao, L., Aubinet, M., Beer, C., Bernhofer, C., Black, K. G., Bonal, D., Bonnefond, J.-M., Chambers, J., Ciais, P., Cook, B., Davis, K. J., Dolman, A. J., Gielen, B., Goulden, M., Grace, J., Granier, A., Grelle, A., Griffis, T., Grünwald, T., Guidolotti, G., Hanson, P. J., Harding, R., Hollinger, D. Y., Hutrya, L. R., Kolari, P., Kruijt, B., Kutsch, W., Lagergren, F., Laurila, T., Law, B. E., Le Maire, G., Lindroth, A., Loustau, D., Malhi, Y., Mateus, J., Migliavacca, M., Misson, L., Montagnani, L., Moncrieff, J., Moors, E., Munger, J. W., Nikinmaa, E., Ollinger, S. V., Pita, G., Rebmann, C., Rouspard, O., Saigusa, N., Sanz, M. J., Seufert, G., Sierra, C., Smith, M.-L., Tang, J., Valentini, R., Vesala, T., and Janssens, I. A.: CO<sub>2</sub> balance of boreal, temperate, and tropical forests derived from a global database, *Glob. Chang. Biol.*, 13, 2509–2537, <https://doi.org/10.1111/j.1365-2486.2007.01439.x>, 2007.

Marushchak, M. E., Kiepe, I., Biasi, C., Elsakov, V., Friborg, T., Johansson, T., Soegaard, H., Virtanen, T., and Martikainen, P. J.: Carbon dioxide balance of subarctic tundra from plot to regional scales, <https://doi.org/10.5194/bg-10-437-2013>, 2013.

McGuire, A. D., Christensen, T. R., Hayes, D. J., Heroult, A., Euskirchen, E., Yi, Y., Kimball, J. S., Koven, C., Lafleur, P., Miller, P. A., Oechel, W., Peylin, P., and Williams, M.: An assessment of the carbon balance of arctic tundra: comparisons among observations, process models, and atmospheric inversions, *Biogeosci. Discuss.*, 9, 4543, <https://doi.org/10.5194/bg-9-3185-2012>, 2012.

McGuire, A. D., Koven, C., Lawrence, D. M., Clein, J. S., Xia, J., Beer, C., Burke, E., Chen, G., Chen, X., Delire, C., Jafarov, E., MacDougall, A. H., Marchenko, S., Nicolsky, D., Peng, S., Rinke, A., Saito, K., Zhang, W., Alkama, R., Bohn, T. J., Ciais, P., Decharme, B., Ekici, A., Gouttevin, I., Hajima, T., Hayes, D. J., Ji, D., Krinner, G., Lettenmaier, D. P., Luo, Y., Miller, P. A., Moore, J. C., Romanovsky, V., Schädel, C., Schaefer, K., Schuur, E. A. G., Smith, B., Sueyoshi, T., and Zhuang, Q.: Variability in the sensitivity among model simulations of permafrost and carbon dynamics in the permafrost region between 1960 and 2009, *Global Biogeochem. Cycles*, 30, 1015–1037, <https://doi.org/10.1002/2016GB005405>, 2016.

Merbold, L., Kutsch, W. L., Corradi, C., Kolle, O., Rebmann, C., Stoy, P. C., Zimov, S. A., and Schulze, E.-D.: Artificial drainage and associated carbon fluxes (CO<sub>2</sub>/CH<sub>4</sub>) in a tundra ecosystem, *Glob. Chang. Biol.*, 15, 2599–2614, <https://doi.org/10.1111/j.1365-2486.2009.01962.x>, 2009.

Mishra, U., Hugelius, G., Shelef, E., Yang, Y., Strauss, J., Lupachev, A., Harden, J. W., Jastrow, J. D., Ping, C.-L., Riley, W. J., Schuur, E. A. G., Matamala, R., Siewert, M., Nave, L. E., Koven, C. D., Fuchs, M., Palmtag, J., Kuhry, P., Treat, C. C., Zubrzycki, S., Hoffman, F. M., Elberling, B., Camill, P., Veremeeva, A., and Orr, A.: Spatial heterogeneity and environmental predictors

of permafrost region soil organic carbon stocks, *Sci Adv*, 7,  
<https://doi.org/10.1126/sciadv.aaz5236>, 2021.

Natali, S. M., Watts, J. D., Rogers, B. M., Potter, S., Ludwig, S. M., Selbmann, A.-K., Sullivan, P. F., Abbott, B. W., Arndt, K. A., Birch, L., Björkman, M. P., Bloom, A. A., Celis, G., Christensen, T. R., Christiansen, C. T., Commane, R., Cooper, E. J., Crill, P., Czimczik, C., Davydov, S., Du, J., Egan, J. E., Elberling, B., Euskirchen, E. S., Friborg, T., Genet, H., Göckede, M., Goodrich, J. P., Grogan, P., Helbig, M., Jafarov, E. E., Jastrow, J. D., Kalhori, A. M., Kim, Y., Kimball, J. S., Kutzbach, L., Lara, M. J., Larsen, K. S., Lee, B.-Y., Liu, Z., Lorant, M. M., Lund, M., Lupascu, M., Madani, N., Malhotra, A., Matamala, R., McFarland, J., McGuire, A. D., Michelsen, A., Minions, C., Oechel, W. C., Olefeldt, D., Parmentier, F.-J. W., Pirk, N., Poulter, B., Quinton, W., Rezanezhad, F., Risk, D., Sachs, T., Schaefer, K., Schmidt, N. M., Schuur, E. A. G., Semenchuk, P. R., Shaver, G., Sonntag, O., Starr, G., Treat, C. C., Waldrop, M. P., Wang, Y., Welker, J., Wille, C., Xu, X., Zhang, Z., Zhuang, Q., and Zona, D.: Large loss of CO<sub>2</sub> in winter observed across the northern permafrost region, *Nat. Clim. Chang.*, 9, 852–857, <https://doi.org/10.1038/s41558-019-0592-8>, [2019](https://doi.org/10.1038/s41558-019-0592-8)[2019a](https://doi.org/10.1038/s41558-019-0592-8).

[Natali, S., J.D. Watts, S. Potter, B.M. Rogers, S. Ludwig, A. Selbmann, P. Sullivan et al. Synthesis of winter in situ soil CO<sub>2</sub> flux in pan-arctic and boreal regions, 1989-2017: \[https://daac.ornl.gov/ABOVE/guides/Nongrowing\\\_Season\\\_CO2\\\_Flux.html\]\(https://daac.ornl.gov/ABOVE/guides/Nongrowing\_Season\_CO2\_Flux.html\), 2019b.](https://doi.org/10.1038/s41558-019-0592-8)

[Nobrega, S. and Grogan, P.: Landscape and ecosystem-level controls on net carbon dioxide exchange along a natural moisture gradient in Canadian low arctic tundra, \*Ecosystems\*, 11, 377–396, <https://doi.org/10.1007/s10021-008-9128-1>, 2008.](https://doi.org/10.1007/s10021-008-9128-1)

Novick, K. A., Biederman, J. A., Desai, A. R., Litvak, M. E., Moore, D. J. P., Scott, R. L., and Torn, M. S.: The AmeriFlux network: A coalition of the willing, *Agric. For. Meteorol.*, 249, 444–456, <https://doi.org/10.1016/j.agrformet.2017.10.009>, 2018.

Nykänen, H., Heikkinen, J. E. P., Pirinen, L., Tiilikainen, K., and Martikainen, P. J.: Annual CO<sub>2</sub> exchange and CH<sub>4</sub> fluxes on a subarctic peat mire during climatically different years, *Global Biogeochem. Cycles*, 17, 2003.

Oechel, W. C., Vourlitis, G. L., Hastings, S. J., Zulueta, R. C., Hinzman, L., and Kane, D.: Acclimation of ecosystem CO<sub>2</sub> exchange in the Alaskan Arctic in response to decadal climate warming, *Nature*, 406, 978–981, <https://doi.org/10.1038/35023137>, 2000.

[Pallandt M., Kumar J., Mauritz M., et al. Representativeness assessment of the pan-Arctic eddy-covariance site network, and optimized future enhancements. \*Biogeosciences Discussions\* \(July\): 1–42, 2021.](https://doi.org/10.5194/bgd-18-1-2021)

Papale, D., Reichstein, M., Aubinet, M., Canfora, E., Bernhofer, C., Kutsch, W., Longdoz, B., Rambal, S., Valentini, R., Vesala, T., and Yakir, D.: Towards a standardized processing of Net Ecosystem Exchange measured with eddy covariance technique: algorithms and uncertainty estimation, *Biogeosciences*, 3, 571–583, <https://doi.org/10.5194/bg-3-571-2006>, 2006.

Paris, J.-D., Ciais, P., Rivier, L., Chevallier, F., Dolman, H., Flaud, J.-M., Garrec, C., Gerbig, C., Grace, J., Huertas, E., Johannessen, T., Jordan, A., Levin, I., Papale, D., Valentini, R., Watson, A., Vesala, T., and ICOS-PP Consortium: Integrated Carbon Observation System, 12397, 2012.

Parker, T. C., Subke, J.-A., and Wookey, P. A.: Rapid carbon turnover beneath shrub and tree vegetation is associated with low soil carbon stocks at a subarctic treeline, *Glob. Chang. Biol.*, 21, 2070–2081, <https://doi.org/10.1111/gcb.12793>, 2015.

Parmentier, F.-J., Sonnentag, O., Mauritz, M., Virkkala, A.-M., and Schuur, E.: Is the northern permafrost zone a source or a sink for carbon?, *Eos*, 100, <https://doi.org/10.1029/2019eo130507>, 2019.

Pastorello, G., Trotta, C., Canfora, E., Chu, H., Christianson, D., Cheah, Y.-W., Poindexter, C., Chen, J., Elbashandy, A., Humphrey, M., Isaac, P., Polidori, D., Ribeca, A., van Ingen, C., Zhang, L., Amiro, B., Ammann, C., Arain, M. A., Ardö, J., Arkebauer, T., Arndt, S. K., Arriga, N., Aubinet, M., Aurela, M., Baldocchi, D., Barr, A., Beamesderfer, E., Marchesini, L. B., Bergeron, O., Beringer, J., Bernhofer, C., Berveiller, D., Billesbach, D., Black, T. A., Blanken, P. D., Bohrer, G., Boike, J., Bolstad, P. V., Bonal, D., Bonnefond, J.-M., Bowling, D. R., Bracho, R., Brodeur, J., Brümmer, C., Buchmann, N., Burban, B., Burns, S. P., Buysse, P., Cale, P., Cavagna, M., Cellier, P., Chen, S., Chini, I., Christensen, T. R., Cleverly, J., Collalti, A., Consalvo, C., Cook, B. D., Cook, D., Coursolle, C., Cremonese, E., Curtis, P. S., D'Andrea, E., da Rocha, H., Dai, X., Davis, K. J., De Cinti, B., de Grandcourt, A., De Ligne, A., De Oliveira, R. C., Delpierre, N., Desai, A. R., Di Bella, C. M., di Tommasi, P., Dolman, H., Domingo, F., Dong, G., Dore, S., Duce, P., Dufrière, E., Dunn, A., Dušek, J., Eamus, D., Eichelmann, U., ElKhidir, H. A. M., Eugster, W., Ewenz, C. M., Ewers, B., Famulari, D., Fares, S., Feigenwinter, I., Feitz, A., Fensholt, R., Filippa, G., Fischer, M., Frank, J., Galvagno, M., Gharun, M., Gianelle, D., et al.: The FLUXNET2015 dataset and the ONEFlux processing pipeline for eddy covariance data, *Sci Data*, 7, 225, <https://doi.org/10.1038/s41597-020-0534-3>, 2020.

Pavelka, M., Acosta, M., Kiese, R., Altimir, N., Brümmer, C., Crill, P., Darenova, E., Fuß, R., Gielen, B., Graf, A., Klemetsson, L., Lohila, A., Longdoz, B., Lindroth, A., Nilsson, M., Marañón-Jimenez, S., Merbold, L., Montagnani, L., Peichl, M., Pihlatie, M., Pumpanen, J., Ortiz, P. S., Silvennoinen, H., Skiba, U., Vestin, P., Weslien, P., Janouš, D., and Kutsch, W.: Standardisation of chamber technique for CO<sub>2</sub>, N<sub>2</sub>O and CH<sub>4</sub> fluxes measurements from terrestrial ecosystems, *Int. Agrophys.*, 32, 569–587, <https://doi.org/10.1515/intag-2017-0045>, 2018.

Phillips, C. L., Bond-Lamberty, B., Desai, A. R., Lavoie, M., Risk, D., Tang, J., Todd-Brown, K., and Vargas, R.: The value of soil respiration measurements for interpreting and modeling terrestrial carbon cycling, *Plant Soil*, 413, 1–25, <https://doi.org/10.1007/s11104-016-3084-x>, 2017.

Pirk, N., Sievers, J., Mertes, J., Parmentier, F.-J. W., Mastepanov, M., and Christensen, T. R.: Spatial variability of CO<sub>2</sub> uptake in polygonal tundra: assessing low-frequency disturbances in eddy covariance flux estimates, *Biogeosciences*, 14, 3157–3169, <https://doi.org/10.5194/bg-14-3157-2017>, 2017.

Raynolds, M. K., Walker, D. A., Balsler, A., Bay, C., Campbell, M., Cherosov, M. M., Daniëls, F. J. A., Eidesen, P. B., Ermokhina, K. A., Frost, G. V., Jedrzejek, B., Jorgenson, M. T., Kennedy, B. E., Kholod, S. S., Lavrinenko, I. A., Lavrinenko, O. V., Magnússon, B., Matveyeva, N. V., Metúsalemsson, S., Nilsen, L., Olthof, I., Pospelov, I. N., Pospelova, E. B., Pouliot, D., Razzhivin, V., Schaepman-Strub, G., Šibík, J., Telyatnikov, M. Y., and Troeva, E.: A raster version of the Circumpolar Arctic Vegetation Map (CAVM), *Remote Sens. Environ.*, 232, 111297, <https://doi.org/10.1016/j.rse.2019.111297>, 2019.

Reichstein, M., Falge, E., Baldocchi, D., Papale, D., Aubinet, M., Berbigier, P., Bernhofer, C., Buchmann, N., Gilmanov, T., Granier, A., Grunwald, T., Havrankova, K., Ilvesniemi, H., Janous, D., Knohl, A., Laurila, T., Lohila, A., Loustau, D., Matteucci, G., Meyers, T., Miglietta, F., Ourcival, J.-M., Pumpanen, J., Rambal, S., Rotenberg, E., Sanz, M., Tenhunen, J., Seufert, G., Vaccari, F., Vesala, T., Yakir, D., and Valentini, R.: On the separation of net ecosystem exchange into assimilation and ecosystem respiration: review and improved algorithm, *Glob. Chang. Biol.*, 11, 1424–1439, <https://doi.org/10.1111/j.1365-2486.2005.001002.x>, 2005.

Riutta, T., Laine, J., Aurela, M., Rinne, J., Vesala, T., Laurila, T., Haapanala, S., Pihlatie, M., and Tuittila, E.-S.: Spatial variation in plant community functions regulates carbon gas dynamics in a boreal fen ecosystem, *Tellus B Chem. Phys. Meteorol.*, 59, 838–852, <https://doi.org/10.1111/j.1600-0889.2007.00302.x>, 2007.

Ryan, M. G., Lavigne, M. B., and Gower, S. T.: Annual carbon cost of autotrophic respiration in boreal forest ecosystems in relation to species and climate, *J. Geophys. Res.*, 102, 28871–28883, <https://doi.org/10.1029/97jd01236>, 1997.

[Schneider, J., Kutzbach, L., and Wilmking, M.: Carbon dioxide exchange fluxes of a boreal peatland over a complete growing season, Komi Republic, NW Russia, \*Biogeochemistry\*, 111, 485–513, https://doi.org/10.1007/s10533-011-9684-x, 2012.](https://doi.org/10.1007/s10533-011-9684-x)

Schuur, E. A. G., McGuire, A. D., Schädel, C., Grosse, G., Harden, J. W., Hayes, D. J., Hugelius, G., Koven, C. D., Kuhry, P., Lawrence, D. M., Natali, S. M., Olefeldt, D., Romanovsky, V. E., Schaefer, K., Turetsky, M. R., Treat, C. C., and Vonk, J. E.: Climate change

and the permafrost carbon feedback, *Nature*, 520, 171–179, <https://doi.org/10.1038/nature14338>, 2015.

Sellers, P. J., Hall, F. G., Kelly, R. D., Black, A., Baldocchi, D., Berry, J., Ryan, M., Ranson, K. J., Crill, P. M., Lettenmaier, D. P., Margolis, H., Cihlar, J., Newcomer, J., Fitzjarrald, D., Jarvis, P. G., Gower, S. T., Halliwell, D., Williams, D., Goodison, B., Wickland, D. E., and Guertin, F. E.: BOREAS in 1997: Experiment overview, scientific results, and future directions, *J. Geophys. Res.*, 102, 28731–28769, <https://doi.org/10.1029/97jd03300>, 1997.

Shaver, G. R., L. E. Street, Rastetter, E. B., M. T. Van Wijk, and Williams, M.: Functional Convergence in Regulation of Net CO<sub>2</sub> Flux in Heterogeneous Tundra Landscapes in Alaska and Sweden, *J. Ecol.*, 95, 802–817, 2007.

Siewert, M. B., Hanisch, J., Weiss, N., Kuhry, P., Maximov, T. C., and Hugelius, G.: Comparing carbon storage of Siberian tundra and taiga permafrost ecosystems at very high spatial resolution: ECOSYSTEM CARBON IN TAIGA AND TUNDRA, *J. Geophys. Res. Biogeosci.*, 120, 1973–1994, <https://doi.org/10.1002/2015jg002999>, 2015.

Soloway, A. D., Amiro, B. D., Dunn, A. L., and Wofsy, S. C.: Carbon neutral or a sink? Uncertainty caused by gap-filling long-term flux measurements for an old-growth boreal black spruce forest, *Agric. For. Meteorol.*, 233, 110–121, <https://doi.org/10.1016/j.agrformet.2016.11.005>, 2017.

Tarnocai, C., Canadell, J. G., Schuur, E. A. G., Kuhry, P., Mazhitova, G., and Zimov, S.: Soil organic carbon pools in the northern circumpolar permafrost region, *Global Biogeochem. Cycles*, 23, 2009.

Tramontana, G., Migliavacca, M., Jung, M., Reichstein, M., Keenan, T. F., Camps-Valls, G., Ogee, J., Verrelst, J., and Papale, D.: Partitioning net carbon dioxide fluxes into photosynthesis and respiration using neural networks, *Glob. Chang. Biol.*, 26, 5235–5253, <https://doi.org/10.1111/gcb.15203>, 2020.

Valentini, R.: EUROFLUX: An Integrated Network for Studying the Long-Term Responses of Biospheric Exchanges of Carbon, Water, and Energy of European Forests, in: *Fluxes of Carbon, Water and Energy of European Forests*, edited by: Valentini, R., Springer Berlin Heidelberg, Berlin, Heidelberg, 1–8, [https://doi.org/10.1007/978-3-662-05171-9\\_1](https://doi.org/10.1007/978-3-662-05171-9_1), 2003.

Virkkala, A.-M., Virtanen, T., Lehtonen, A., Rinne, J., and Luoto, M.: The current state of CO<sub>2</sub> flux chamber studies in the Arctic tundra: A review, *Progress in Physical Geography: Earth and Environment*, 42, 162–184, <https://doi.org/10.1177/0309133317745784>, 2018.



Virkkala, A.-M., Abdi, A. M., Luoto, M., and Metcalfe, D. B.: Identifying multidisciplinary research gaps across Arctic terrestrial gradients, *Environ. Res. Lett.*, 14, 124061, <https://doi.org/10.1088/1748-9326/ab4291>, 2019.

~~Virkkala, A.-M., Virkkala, A.-M., Natali, S., Rogers, B. M., Watts, J. A., Savage, K., Connon, S. J., Mauritz, M., Schuur, E. A. G., Peter, D., and Minions, C. et al.: The ABCflux Database: Arctic-Boreal CO<sub>2</sub> Flux Observations Aggregated to Monthly Time Steps, ORNL-DAAC, Oak Ridge, Tennessee, USA, <https://doi.org/10.3334/ORNLDAAC/1934>, 2021a.~~

~~Virkkala, A.-M., Aalto, J., Rogers, B. M., Tagesson, T., Treat, C. C., Natali, S. M., Watts, J. D., Potter, S., Lehtonen, A., Mauritz, M., Schuur, E. A. G., Kochendorfer, J., Zona, D., Oechel, W., Kobayashi, H., Humphreys, E., Goeckede, M., Iwata, H., Lafleur, P. M., Euskirchen, E. S., Bokhorst, S., Marushchak, M., Martikainen, P. J., Elberling, B., Voigt, C., Biasi, C., Sonntag, O., Parmentier, F.-J. W., Ueyama, M., Celis, G., St Loius, V. L., Emmerton, C. A., Peichl, M., Chi, J., Järveoja, J., Nilsson, M. B., Oberbauer, S. F., Torn, M. S., Park, S.-J., Dolman, H., Mammarella, I., Chae, N., Poyatos, R., López-Blanco, E., Røjle Christensen, T., Jung Kwon, M., Sachs, T., Holl, D., and Luoto, M.: Statistical upscaling of ecosystem CO<sub>2</sub> fluxes across the terrestrial tundra and boreal domain: regional patterns and uncertainties, *Glob. Chang. Biol.*, <https://doi.org/10.1111/gcb.15659>, 2021b.~~

~~Virkkala, A.-M., Natali, S., Rogers, B. M., Watts, J. A., Savage, K., Connon, S. J., Mauritz, M., Schuur, E. A. G., Peter, D., Minions, C. et al.: The ABCflux Database: Arctic-Boreal CO<sub>2</sub> Flux and Site Environmental Data, 1989-2020, <https://doi.org/10.3334/ORNLDAAC/1934>, 2021a.~~

Voigt, C., Lamprecht, R. E., Marushchak, M. E., Lind, S. E., Novakovskiy, A., Aurela, M., Martikainen, P. J., and Biasi, C.: Warming of subarctic tundra increases emissions of all three important greenhouse gases - carbon dioxide, methane, and nitrous oxide, *Glob. Chang. Biol.*, 23, 3121–3138, <https://doi.org/10.1111/gcb.13563>, 2017.

Wang, K., Liu, C., Zheng, X., Pihlatie, M., Li, B., Haapanala, S., Vesala, T., Liu, H., Wang, Y., Liu, G., and Hu, F.: Comparison between eddy covariance and automatic chamber techniques for measuring net ecosystem exchange of carbon dioxide in cotton and wheat fields, *Biogeosciences*, 10, 6865–6877, <https://doi.org/10.5194/bg-10-6865-2013>, 2013.

Wang, L., Lee, X., Wang, W., Wang, X., Wei, Z., Fu, C., Gao, Y., Lu, L., Song, W., Su, P., and Lin, G.: A Meta-Analysis of Open-Path Eddy Covariance Observations of Apparent CO<sub>2</sub> Flux in Cold Conditions in FLUXNET, *J. Atmos. Ocean. Technol.*, 34, 2475–2487, <https://doi.org/10.1175/JTECH-D-17-0085.1>, 2017.

~~Wutzler, T., Lucas-Moffat, A., Migliavacca, M., Knauer, J., Sickel, K., Šigut, L., Menzer, O., and Reichstein, M.: Basic and extensible post-processing of eddy covariance flux data with REddyProc, *Biogeosciences*, 15, 5015–5030, <https://doi.org/10.5194/bg-15-5015-2018>, 2018.~~

